Rossby Centre Newsletter

May 2009

The Rossby Centre is the climate research unit of the Swedish Meteorological and Hydrological Institute, SMHI. This Newsletter aims to provide useful information to stakeholders and researchers on climate change regarding present research activities at the Rossby Centre.

In a slight change to earlier versions of the Rossby Centre Newsletter, the Newsletter now includes a number of relatively detailed articles, describing ongoing research at the Rossby Centre. Each article is described in a short summary form at the beginning of the Newsletter so the reader can decide if the more detailed version is of interest to them. The Newsletter also includes general staff information, details of the 2009 Rossby Centre Day and information on a new, international effort to provide globally coordinated downscaled climate scenarios for all land regions of the globe. This initiative is referred to as CORDEX and is introduced on page 3.

1. Rossby Centre Day 2009

This year's Rossby Centre Day will be at SMHI, Norrköping on October 21 with the subject: **Using Regional Climate Scenarios in impact and adaptation studies.** During the day we will present the latest climate scenario results from the Rossby Centre. The main theme of the day will be to discuss new and established techniques for further downscaling/manipulating Regional Climate Model (RCM) output into a form of greater direct utility in impact and adaptation work. Examples of this work and subsequent use of RCM results in climate impact assessment will be presented.

A formal invitation to the Rossby Day will be sent out later in the year. For now please record this date in your diary and if you would like to register in advance send a mail to Rossby.Data@smhi.se

2. Summary of Articles

Understanding the time-axis in coupled climate models: Uncertainty, natural variability and the need for an ensemble approach

This article explains how the calendar date in a coupled climate model should be understood. It further explains why it is not reasonable to expect the simulation of natural variability in such a model to follow the same time evolution as seen in observations. This implies that it is not possible simply to compare the time evolution of the simulated climate against observations, more sophisticated methods are required to evaluate the model's performance. The article further goes on to discuss the role of natural variability in limiting our ability to tightly constrain estimates of future climate change and why this problem is larger both for the near future and for smaller spatial scales.

Read the full article on page 3.

Changes in the wintertime temperature climate as deduced from an ensemble of regional climate change simulations for Europe

At the Rossby Centre an ensemble of transient regional climate change scenarios has been produced. The scenarios cover the time period 1961-2100 and allow us to address uncertainties related to emission scenarios, choice of global model for providing boundary conditions, horizontal resolution, and natural variability. Altogether 18 140-year scenarios have been completed so far.

The results show large differences in the simulation of the recent past climate (1961-1990) depending on choice of global climate model and internal natural variability. Compared to observational data sets the ensemble mean performs better than most individual scenarios. For the relatively near future (2011-2040) the results show a large contribution from natural variability to the overall uncertainty in the climate change signal. By the end of the century (2071-2100), the overall uncertainty is more dominated by choice of global climate model and emission scenario.

Read the full article on page 9.

First Regional Arctic Climate Scenarios with coupled RCAO

Global climate models show large discrepancies in predictions of present and future climate in the Arctic, and consequently, large uncertainties. In order to reduce the uncertainties, a number of regional Arctic scenario experiments are performed with the Rossby Centre Atmosphere Ocean climate model (RCAO) using global model data as lateral boundary forcing.

The results from these future simulations show that the variations in the Arctic between the regional simulations and the corresponding global simulation are of the same order of magnitude than those between different global simulations. Furthermore, different representations of the regional model show locally significant changes in the predicted climate change. Generally, the large scale change pattern and the dominating trends are governed by the global simulations. However, the regional simulations show in specific regions such as the Barents Sea a stronger and faster climate response to climate change. Sea ice variations are much stronger with several rapid change events and partial recoveries in the 21st century than in the global simulations.

This leads to the conclusion that regional coupled simulations provide important additional information of potential climate change in the Arctic and thus are important for impact studies and adaptation and mitigation strategies.

Read the full article on page 15.

Performance of RCA3 and RCA3.5 over South America

Rossby Centre is a partner of the EC 7th framework project CLARIS la Plata basin (CLARIS LPB). Within the context of this multidiciplinary South American – Europe project, Rossby Centre will contribute with regonal climate change scenarios for the South American continent that will be used for impact and adaptation studies of water resources, hydropower and ecological systems. Partly motivated by this project, the Rossby Centre regional atmospheric model has been adapted for tropical regions. Here we present some results from a comparison between the performance of RCA3-E and RCA3.5 with 24 and 40 vertical levels over the continent.

Read the full article on page 17.

Simulating Precipitation over Africa with a new version of RCA

This article describes the first attempt to use an updated version of the Rossby Centre Atmospheric Regional Climate Model, RCA3.5, to simulate climate variability over Africa. In the article we describe the ability of RCA3.5 to simulate precipitation variability over the entire African continent, when the model is forced by the new ERA-interim reanalysis data set from ECMWF. This activity is an initial step in evaluating RCA3.5 before utilizing it to generate future climate scenarios over Africa forced by results from a range of Global Climate Model simulations.

Read the full article on page 20.

3. CORDEX: A Coordinated Regional Downscaling Experiment

by Colin Jones

Under the direction of the World Climate Research Program (WCRP), the international Regional Climate Modelling and Downscaling community is developing a plan to better coordinate activities in Regional Climate Modelling, Statistical Downscaling and the provision of climate scenarios to the user community. This activity aims to link with the 5th Coupled Model Intercomparison Project (CMIP5), using a subset of the CMIP5 Global Climate Model (GCM) simulations as boundary conditions for subsequent downscaling. WCRP has established a Task Force for Regional Climate Downscaling (TFRCD) that met with around 50 experts at a meeting in Toulouse in February 2009. A second meeting occurred at the Regional Climate conference held in Lund, Sweden May 4th-8th 2009.

This group is beginning to define a number of Limited Area domains, centred on areas of interest covering most of the land regions of the globe. The aims are three-fold;

(i) To define domains, boundary conditions and simulated variables to evaluate the performance of RCMs in a common manner for a range of climatic regions.

(ii) To develop a matrix of regional climate scenarios for a large number of regions of the world. This matrix should sample the majority of the sources of uncertainty involved in developing regional climate scenarios, including sampling a range of Global Climate Simulations as boundary conditions that encompass a number of greenhouse gas emission scenarios. For each GCM boundary condition data set a number of Regional Climate Models (RCMs) should be applied.

(iii) To better engage developing nation scientists in the generation and use of regional climate scenarios and to improve the accessibility of this data for the impact and adaptation communities.

A common RCM resolution of 50km has been agreed, with groups encouraged to explore the benefits of increased resolution where possible. Groups are encouraged to run their RCMs over a number of the predefined regions either in transient mode (e.g. 1950-2100) or in time slice mode, where the time slices in order of preference are (i)1980-2010, (ii) 2040-2070, (iii) 2010-2040, (iv) 2070-2100 and (v) 1950-1980. An important aspect of this effort is to ensure that the RCM scenarios are readily useable by the climate impacts and adaptation community, through use of a common set of stored data in a common format and to make this data easily accessible.

It was decided that an initial focus for generating regional climate scenarios would be Africa, with as many groups as possible encouraged to downscale at least 1 GCM scenario from the CMIP5 experiment. If possible a range of GCMs, emission scenarios and RCM downscaled climates, will be made available, covering the entire African continent, within the timescale of the 5th Intergovernmental Panel on Climate Change (IPCC) Assessment Report. Other regions of the world will be addressed in a coordinated fashion more gradually over the coming years.

4. Understanding the time-axis in coupled climate models: Uncertainty, natural variability and the need for an ensemble approach

by Colin Jones and Grigory Nikulin

1. Introduction

In this article we aim to explain how one can best utilize future climate scenarios that are a result of downscaling coupled Atmosphere-Ocean Global Climate Models (AOGCMs). We wish to explain the way in which calendar time should be understood in relation to these simulations and thereby, when and where it is appropriate to compare downscaled Regional Climate Model (RCM) results as a function of real calendar time, especially in relation to observational data. We further aim to explain the role natural variability plays in this problem and in limiting our ability to tightly define future climate conditions. This discussion highlights why an ensemble approach is necessary in simulating regional climate change.

2. Simulating the observed climate: Natural variability and the concept of model calendar time

The majority of Climate Scenarios produced with the Rossby Centre Regional Climate Model (RCA, Jones et al. 2004, Kjellström et al. 2005) cover the period 1961-2100, with the lateral and surface boundary conditions derived from a range of coupled AOGCMs. For most scenario runs the AOGCMs have a nominal start date of ~1860. Generally, it is at this date that the atmospheric greenhouse gas (GHG) concentrations prescribed in the AOGCMs increase above 'pre-industrial' values, following an observational based increase up to present-day and then one of a range of future emissions scenarios thereafter. An important requirement is that at the nominal start date of 1860 the coupled AOGCM should be full spun-up to its simulated climatological state, with in particular the deep ocean circulation fully developed and ocean-atmosphere fluxes internally balanced. In practice this means there should be as little temporal drift as possible in global mean variables such as; surface temperature, precipitation minus evaporation and top of the atmosphere net radiation fluxes. To achieve this state the AOGCM is started either from isothermal conditions and a resting state, or from some estimate of the ocean and atmospheric state based on an observed climatology. The model is then integrated forwards in time for many hundreds of simulated years with the only external forcing being prescribed values of GHGs, aerosols, solar constant and land-use/vegetation cover, all representative of pre-industrial conditions, along with the observed rotation rate of the Earth.

If one assumes that a given AOGCM takes one thousand simulated years to come into balance (a not unreasonable figure for the ocean thermohaline circulation), then in terms of the model calendar, the spin-up phase of the AOGCM integration begins at the year 860A.D. Clearly no observations are available to initialize the model at this date. Hence, in terms of the AOGCMs initial conditions, the date is completely arbitrary. Throughout the thousand-year spin up run, the model is forced by constant values of GHG concentrations, aerosols, solar forcing and land-use/vegetation, which is clearly a radical oversimiplification of the real (time-varying) external forcing of the climate system over this time-period. From this forcing, a good AOGCM will begin to simulate the climatological conditions observed on Earth, as well as aspects of the observed natural variability. Due to the arbitrary nature of the inital date of the model spin-up, it is important to appreciate that while the AOGCM may successfully simulate many aspects of the observed natural variability, there is no reason to expect this simulated variability to occur in temporal phase with reality (i.e. that the modelled and observed natural variability occur at similar points in the calendar). This important point remains true even when the AOGCM simulation reaches the (nominal) date 1860, at which point GHG concentrations are allowed to increase and we begin to talk about the model simulating the observed climate record, including any anthropogenic induced trends. The only thing tying the AOGCM simulation to a real calendar date is the increasing concentration of GHGs, possibly aerosols and a prescribed land-use/vegetation distribution.

In order to sample the possible range of natural variability in the coupled climate system, AOGCM groups generally choose a range of instantaneous (balanced) states from the latter period of the spin-up run of their AOGCM. These model 'snap-shots' are used as initial conditions for an ensemble of 20th Century runs, all starting at 1860. It is normal to select initial conditions from the spin-up run that are sufficiently different to sample a large fraction of the simulated natural variability in the coupled climate system. One should view this range of initial states as an inherent uncertainty in our ability to know at what phase of the Earth's cycles of natural variability reality actually was in 1860. As these initial conditions can be from any simulated calendar date of the spin-up run, it is clear that the initial date of 1860 is meaningless from the perspective of the Earth's true natural variability.

Run in the manner outlined above we can now appreciate that it is reasonable to expect AOGCMs to;

(i) Simulate the range of natural variability observed in the climate system, *without expecting this to be simulated correctly in time.*

(ii) Simulate any long-term trends in the climate due to increasing concentrations of GHGs *(i.e. the anthropogenic climate change signal).*

Point (ii) has been confirmed by the AOGCM community where coupled models have been run with observed GHG concentrations, solar variability and volcanic forcing for the 20th century and succesfully reproduce the observed trend in global mean temperatures. Repeating the same 20th century runs with identical models, initial conditions and time-varying solar variability and volcanic forcing, but *time-invariant* 'pre-industrial' GHG concentrations, the AOGCMs fail to reproduce the observed trend in the global mean temperature, in particular failing to simulate the observed warming trend since ~1960 (See Stott et al. 2000, IPCC 2007).

On smaller spatial scales natural variability has a larger signal. This can easily be understood if one takes the example of winter temperatures over southern Sweden, which are highly sensitive to atmospheric circulation conditions, such as the strength and frequency of westerly flow from the Atlantic into Southern Sweden. On longer timescales such circulation variability is strongly influenced by the North Atlantic Oscillation (NAO, Hurrell et al. 2001). If it is not possible to compare the time evolution of downscaled results from an AOGCM directly against observations what can we do to evaluate the model's simulated natural variability? Instead, one can compare the power and frequency of the simulated variability around the model's mean conditions over a suitably long averaging period (30 years is often used as a minimum period). Another approach is to select various phases of natural variability (say the positive and negative phases of the NAO) and evaluate whether simulated anomalies in the climate around the model's mean climate are of similar character to the observed anomalies, also grouped into the respective phases of the NAO.

3. Simulating future climate: The role of uncertainty and natural variability

As AOGCMs simulate climate conditions out towards the end of the 21st Century the forced climate change signal, associated with increased GHGs, becomes larger than the signature of natural variability. This is often referred to as the signal to noise ratio. What this actually means is that the signal of forced climate change (e.g. global mean surface temperatures) is now larger than the variability of the global mean surface temperatures due to (i) sampling a range of AOGCMs (relating to our imperfect ability to model the climate system) and (ii) sampling one AOGCM and a range of initial conditions (uncertainty due to natural variability). The point where the forced signal becomes larger than natural variability generally occurs earlier, the larger the spatial area under consideration. Uncertainty in the actual state of the climate as a result of our inability to know where the system is with respect to natural variability remains similar at this point, it is simply that the forced signal is now larger than this uncertainty.

To illustrate this point, figure 1 shows results from 3 integrations of the RCA3 model, each forced by a different ensemble member of the ECHAM5/OM1 AOGCM (Roeckner et al. 2005, Jungclaus et al. 2006) using the SRES A1B GHG emission scenario (Nakicenovic et al. 2000). The only difference between the 3 ECHAM5 runs is the initial conditions used for the model in 1860. RCA3 downscaled the ECHAM5 run for the entire period 1961-2100. In Figure 1 we show the seasonal mean surface temperature for summer and winter, spatially averaged over Southern Sweden. Results are shown for the periods 1980-2000, 2015-2035 and 2070-2090 for each of the 3 ensemble members, while the green line shows the 20 year mean temperature for southern Sweden averaged across the 3 ensemble members.

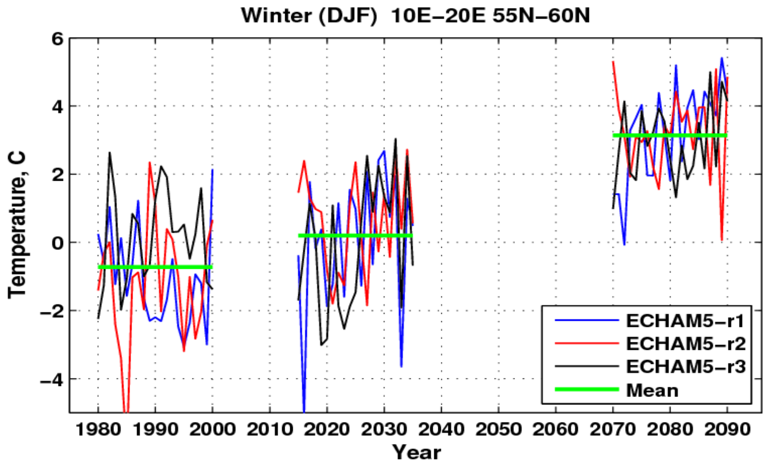

Figure 1a. *RCA3 simulated winter surface temperature for Southern Sweden from 3 members of the ECHAM5 A1B ensemble. Seasonal mean temperatures are shown for each ensemble member for 3 sections of the transient integration from 1950-2100. The green line shows the ensemble mean, 20-year mean temperature for each period.*

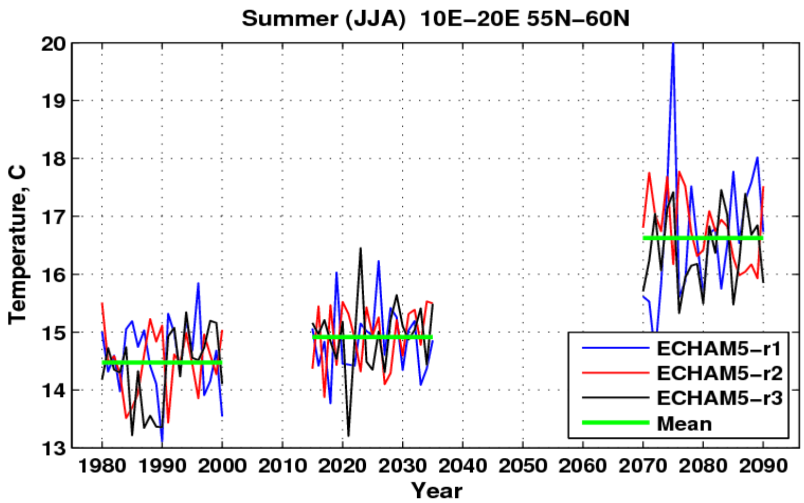

Figure 1b. *As in figure 1a but for the summer season.*

From figure 1 it is clear that at this spatial scale the seasonal mean temperatures simulated by the 3 ensemble members are completely uncorrelated in time. By the decade of the 2020's the mean climate change signal, as shown by the change in the position of the green line in figure 1, is clearly smaller than the variability between the 3 members for the period 1980-2000. Towards the end of the century the mean climate change signal, compared to the period 1980-2000, is now large enough to be distinguished from the inter-ensemble spread. Nevertheless, the ensemble spread remains significant and uncorrelated in time. Generally, simulated winter season variability is larger than in summer, although towards the end of the 21st century, winter variability appears to decrease while the summer variability actually increases somewhat. The former decrease is likely associated with decreased snow cover and the reduction of extremely cold days in the future, while the summer increase may be associated with larger inter-annual variability in summer soil moisture.

Figure 1 clearly shows that the 3 downscaled realizations of the ECHAM5 A1B scenario can at times simulate extended periods (e.g decades or more) of quite different climate change signals over Southern Sweden. As an example, compare in figure 1a the implied trend in winter temperatures for the decade of the 1990's compared to the 2020's in the red (r2) and black (r3) lined ensemble members. Member r2 would suggest a warming over southern Sweden of around 2°C while member r3 indicates a cooling of 1-2°C over this same 30 year period. These differences largely arise as a result of different large scale circulation patterns in the North-East Atlantic-European region, that reflect natural variability in the state of the coupled system in this region.

To illustrate this point further figure 2a shows the simulated change in near surface temperature from each RCA3 member for a 30-year period centred on 2025, relative to a 30-year control period centred on 1985. Figure 2b shows the change in mean sea level pressure (MSLP) over the same period.

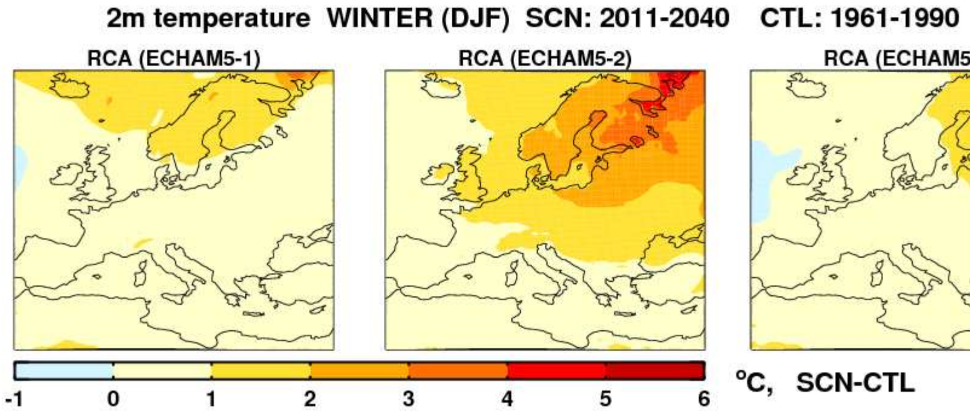

Figure 2a. *Winter season near surface temperature changes for the 30-year period 2011-2040 minus 1961-1990 as simulated by 3 RCA3 simulations forced by 3 members of the ECHAM5 A1B ensemble.*

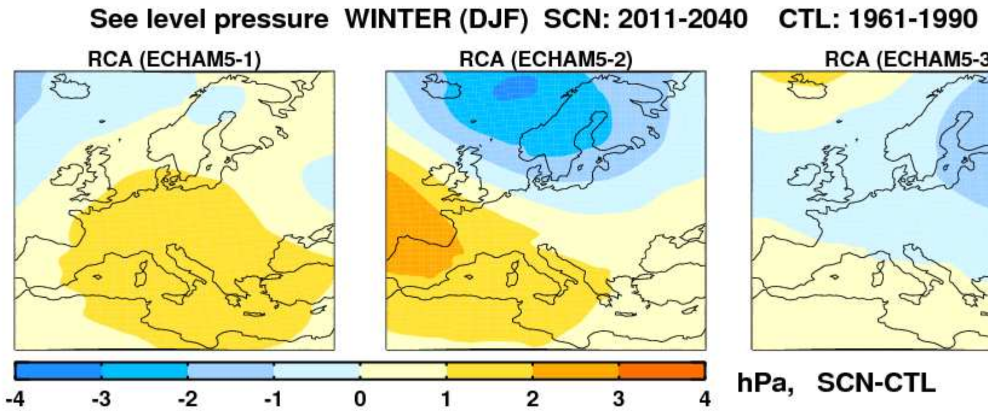

Figure 2b. *As in figure 2a but for simulated mean sea level pressure change.*

Ensemble member 2 simulates increased high pressure over southern Europe and the Atlantic region of the Azores. This can be understood as an intensification and poleward expansion of the Azores anticyclone. In the north Atlantic, MSLP is simulated to decrease. This overall pattern is analogous to an increase in the positive phase of the NAO, (Hurrel 2001). The resulting change in atmospheric circulation sees an increase in westerly flow from the Atlantic into Northern Europe and a significant winter warming, as seen in figure 2a. In contrast, ensemble member 3 shows no change in the Azores high and a weak decrease in MSLP over the north-east corner of the RCA3 domain. The resulting circulation change is a weak increase in northerly flow over southern Sweden and an insignificant change in the winter temperatures. As these changes in circulation are largely a reflection of the system's natural variability, it is impossible to state with any confidence which circulation change is more likely to occur in the future, both are equally likely. This limits our ability to place tight bounds on estimates of regional climate change. Presently, the best method to reduce this uncertainty is to utilize as large an ensemble of simulations as possible. This allows an investigation as to whether certain circulation changes are simulated more frequently than others in the future, allowing a probability of occurrence to be attached to each outcome. This technique is widely used in the area of seasonal prediction (Peng et al. 2002).

4. Conclusions

In this article we have explained the method by which coupled climate models simulate the pre-industrial, present and future climate periods on Earth and how one should understand the simulated date in these simulations. From this explanation we indicated that it is not possible to expect an AOGCM to simulate the natural variability of the climate in temporal phase with observations. In contrast, it ***is*** reasonable to expect a model to simulate the power spectrum and frequency of occurrence of various states of natural variability, just that there is no reason to expect these states to be located correctly in time. This implies that simply comparing the time evolution of a given variable against the observed time evolution is not possible. This statement is increasingly true the larger natural variability is, which generally increases as the spatial area of interest decreases. Instead more sophisticated approaches are required to evaluate the representation of natural variability in an AOGCM, or from RCM downscaled results of an AOGCM. We further illustrated the large role natural variability plays in limiting our ability to constrain estimates of future regional climate change, particularly on shorter timescales where uncertainty due to natural variability can be as large, or larger, than the signal due to anthropogenic climate change. This latter point illustrates the need for an ensemble approach to regional climate modelling, whereby all the inherent sources of uncertainty in future climate conditions (e.g. GCM formulation, GHG emission scenarios, RCM formulation and natural variability) can be sampled and a probabilistic approach be assigned to the various possible evolutions of the climate over the coming 20-100 years. Such an approach to generating regional climate scenarios is being actively pursued at the Rossby Centre. An article discussing initial results from the large ensemble of RCA3 climate scenarios over Europe appears in this Newsletter on page 9.

References

Hurrell, J.W., Y.Kushnir and M.Visbeck 2001. The North Atlantic Oscillation. *Science* **26**, 5504, 603-605

IPCC 2007: Climate Change 2007: The Physical Science Basis. *Contribution of Working Group I to the Fourth Assessment Report of the Intergovernmental Panel on Climate Change* [Solomon, S., et al., eds.]. Cambridge University Press, Cambridge, United Kingdom and New York, NY, USA, 940 pp.

Jones, C. G., Willén, U., Ullerstig, A. and Hansson, U. 2004. The Rossby Centre Regional Atmospheric Climate Model Part I: Model Climatology and Performance for the Present Climate over Europe. *Ambio* **33**:4-5, 199-210.

Jungclaus, J.H., N. Keenlyside, M. Botzet, H. Haak, J.-J. Luo, M. Latif, J. Marotzke, U. Mikolajewicz und E. Roeckner, 2006: Ocean circulation and tropical variability in the coupled model ECHAM5/MPI-OM. *J. Climate*, **19**, 3952-3972

Kjellström, E., Bärring, L., Gollvik, S., Hansson, U., Jones, C., Samuelsson, P., Rummukainen, M., Ullerstig, A., Willén U. and Wyser, K., 2005. A 140-year simulation of European climate with the new version of the Rossby Centre regional atmospheric climate model (RCA3). *Reports Meteorology and Climatology* **108**, SMHI, SE-60176 Norrköping, Sweden, 54 pp

Nakicenovic, N., Alcamo, J., Davis, G., de Vries, B., Fenhann, J., Gaffin, S., Gregory, K., Grübler, A., Jung, T.Y., Kram, T., La Rovere, E.L., Michaelis, L., Mori, S., Morita, T., Pepper, W., Pitcher, H., Price, L., Riahi, K., Roehrl, A., Rogner, H.-H., Sankovski, A., Schlesinger, M., Shukla, P., Smith, S., Swart, R., van Rooijen, S., Victor, N., Dadi Z. (2000): *IPCC Special Report on Emissions Scenarios*. Cambridge University Press, Cambridge, United Kingdom and New York, NY, USA. 599pp.

Peng P., A.Kumar, H. van den Dool and A.G.Barnston (2002) An analysis of multi-model ensemble predictions for seasonal climate anomalies. *J. Geophys. Res*. **107**(D23), 4710, doi:10.1029/2002JD002712.

Roeckner, E., R.Brokopf, M.Esch., M.Giorgetta, S.Hagemann, L.Kornblueh, E.Manzini, U.Schlese, U.Schulzweida, 2006. Sensitivity of Simulated Climate to Horizontal and Vertical Resolution in the ECHAM5 Atmosphere Model. *Journal of Climate* **19** 3771–3791.

Stott P.A, S.F.B.Tett, G.S.Jones, M.R.Allen, J.F.B.Mitchell and G.Jenkins 2000. External Control of the 20th Century Temperature by Natural and Anthropogenic Forcings. *Science* **290**, 5499, 2133-213

5. Changes in wintertime temperature climate as deduced from an ensemble of regional climate change simulations for Europe

by Erik Kjellström, Ulf Hansson, Colin Jones, Grigory Nikulin, Gustav Strandberg and Anders Ullerstig

1. Introduction

In a previous issue of Rossby Centre Newsletter (June 2008), we described the creation of an ensemble of regional climate change scenarios at the Rossby Centre. Since then more simulations have been undertaken and we now have an ensemble that can be used to address questions related to the following uncertainties in future climate change scenarios:

i. how will the external forcing of the climate system change in the future?

ii. how will these changes in external forcing factors influence climate?

iii. to what degree is the future climate change signal masked/amplified by natural variability of the climate system?

The common way to deal with these uncertainties is to perform several simulations constituting an ensemble. Earlier attempts to do this on the regional scale have been pursued in the European projects PRUDENCE (*e.g*. Déqué *et al.*, 2007) and ENSEMBLES (Hewitt and Griggs, 2005). The ensemble can be used to illustrate the uncertainties on the regional scale or to produce probabilistic climate change information in a region. The specific uncertainties i)-iii) are handled in a similar way. This includes using several different emission scenarios to get a grip on the uncertainty related to external forcing thereby sampling a multitude of possible outcomes (Nakićenović *et al*., 2000). Likewise, by using multiple climate models or an ensemble of simulations with one model perturbed in its formulation of the physics, parts of the uncertainties related to how changes in forcing influence the climate can be assessed (*e.g*. Meehl *et al.*, 2007, Murphy *et al.*, 2007). Finally, to get a grip on the natural variability one may use several simulations with one climate model under the same emission scenario differing only in initial conditions.

2. The Rossby Centre regional climate change ensemble

At the Rossby Centre an ensemble of regional climate change scenarios is produced (Table 1). We use the regional climate model RCA3 (Kjellström *et al.*, 2005) to dynamically downscale several experiments with global coupled atmosphere-ocean general circulation models (AOGCMs). The AOGCMs, in turn, are forced by different emission scenarios from the special report on emission scenarios by the IPCC (Nakićenović *et al*. 2000). One AOGCM (ECHAM5/MPI-OM), Jungclaus et al. 2007) has been used to simulate one emission scenario three times differing only in initial conditions to sample some of the natural variability. Another AOGCM (HadCM3) has been run with three different parameter settings to sample some of the uncertainty related to model formulation. That particular ensemble of three simulations includes the reference version of the HadCM3 model and one that has a high sensitivity to changes in the radiative forcing (labelled “high” in the following) and one that has a low sensitivity (low). In addition to all simulations driven by boundary conditions from AOGCMs we also use results from a simulation in which RCA3 got boundary conditions from the reanalysis product ERA40 (Uppala *et al.*, 2005).

Table 1. *Simulations in the regional climate change ensemble at the Rossby Centre. Planned simulations are marked in italics.*

No	**AOGCM** (Institute, country)		**Emission scenario**	**Horisontal resolution** (km)	**Reference**
1	Arpège (CNRM, France)		A1B	50	Déqué et al (1994), Royer et al (2002)
2 3	BCM (NERSC, Norway)		A1B	50 25	Déqué et al (1994), Bleck et al (1992)
4 5 6	CCSM3 (NCAR, USA)		A2 A1B B2	50 50 50	Collins et al (2006)
7 8	ECHAM4 (MPI-met, Germany)		A2 B2	50 50	Roeckner et al (1999)
9	ECHAM5 (MPI-met, Germany)		A2	50	Roeckner et al (2006), Jungclaus et al (2006)
10 11 12 13 *14*			A1B	50 50 50 25 *12.5*	
15			B1	50	
16 17 18 19	HadCM3 (Hadley Centre, UK)	ref (Q0) low (Q3) high (Q16) low (Q3)	A1B	50 50 50 25	Gordon et al (2000)
20	*IPSL-CM4 (IPSL, France)*		*A1B*	*50*	*Hourdin et al (2006)*

3. Results

There are large differences between the simulations in the recent past climate related to internal variability and to choice of AOGCM (Fig. 1). In general these two sources of uncertainty are difficult to distinguish from each other. Here, the three-member ensemble of ECHAM5-driven simulations allows us to look at natural variability alone. Large differences between these three simulations can be seen in some regions but the differences related to choice of AOGCM are generally larger. Part of the biases in temperature can be attributed to the large-scale circulation as indicated by the mean sea level pressure (MSLP). Several of the models show a too low pressure over the British Isles reaching eastwards over the continent and some a too high pressure in the southernmost part of the model domain. This indicates stronger than observed north-south pressure gradient in the area leading to overestimated transport of mild air from the oceans to the continent. The most notable example is the CCSM3-forced run that consequently shows the largest bias in temperature. As a contrast, the low-sensitivity simulation with HadCM3 shows an underestimated N-S MSLP-gradient and too low temperatures in most areas. Compared to most other simulations the best performance is found for the ERA40-driven downscaling. This is expected as the boundary conditions in this case are close to the observed state of the atmosphere. But, some of the other simulations perform equally, or even better, in this season. Also the ensemble mean performs better than most, but not all, individual models although large regional biases in some simulations are seen also in the ensemble mean.

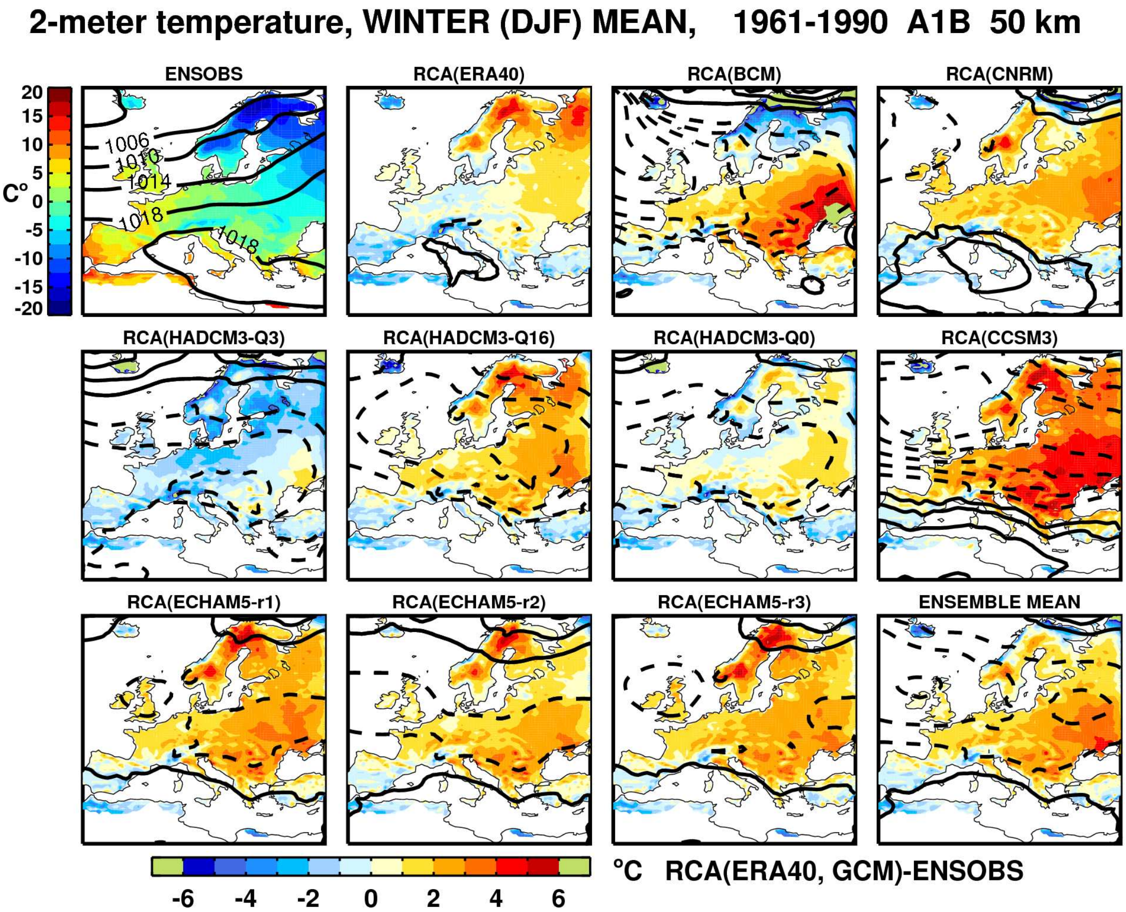

Figure 1. *2m-temperature and mean sea level pressure (contours) in winter (DJF) in the 1961-1990 period. The uppermost left panel shows the ENSEMBLES gridded observational 2m-temperatures (Haylock et al. 2008) and the ERA40 MSLP (Uppala et al. 2005). The one labeled RCA3(ERA40) shows biases compared to the uppermost left panel in an ERA40 downscaling simulation with RCA3. The other panels show biases from the individual 50km A1B-simulations listed in Table 1. The mean (lower right) is taken over the ensemble consisting of 5 simulations with different AOGCMs in the two rightmost columns. MSLP biases are shown for every 2 hPa except 0 (dashed for negative numbers).*

Also in the future climate large differences between the different ensemble members are clearly identifiable (Fig 2). The strongest response is seen in the HadCM3-forced simulations with high climate sensitivity (Q16 in the figure). However, part of the strong response relates to the change in MSLP (higher pressure over the continent and lower over the North Atlantic) leading to more southerly wind bringing warmer air from the south. The ensemble mean shows the strongest increase in northeastern Europe which is the common picture in most scenarios due to the feedback from vanishing snow and ice in this region (*e.g.* Christensen *et al.*, 2007). The MSLP changes also reveal that part of the excess warming in the north may be explained by a stronger transport of mild air from the North Atlantic towards Scandinavia as the north-south pressure gradient increases. The role of natural variability is relatively modest at this time as can be inferred from the three ECHAM5-forced simulations that differ only little from each other. Instead, the overall uncertainty is to a large degree dominated by the choice of AOGCM and the choice of emission scenario (the latter is not shown here) by the end of the century.

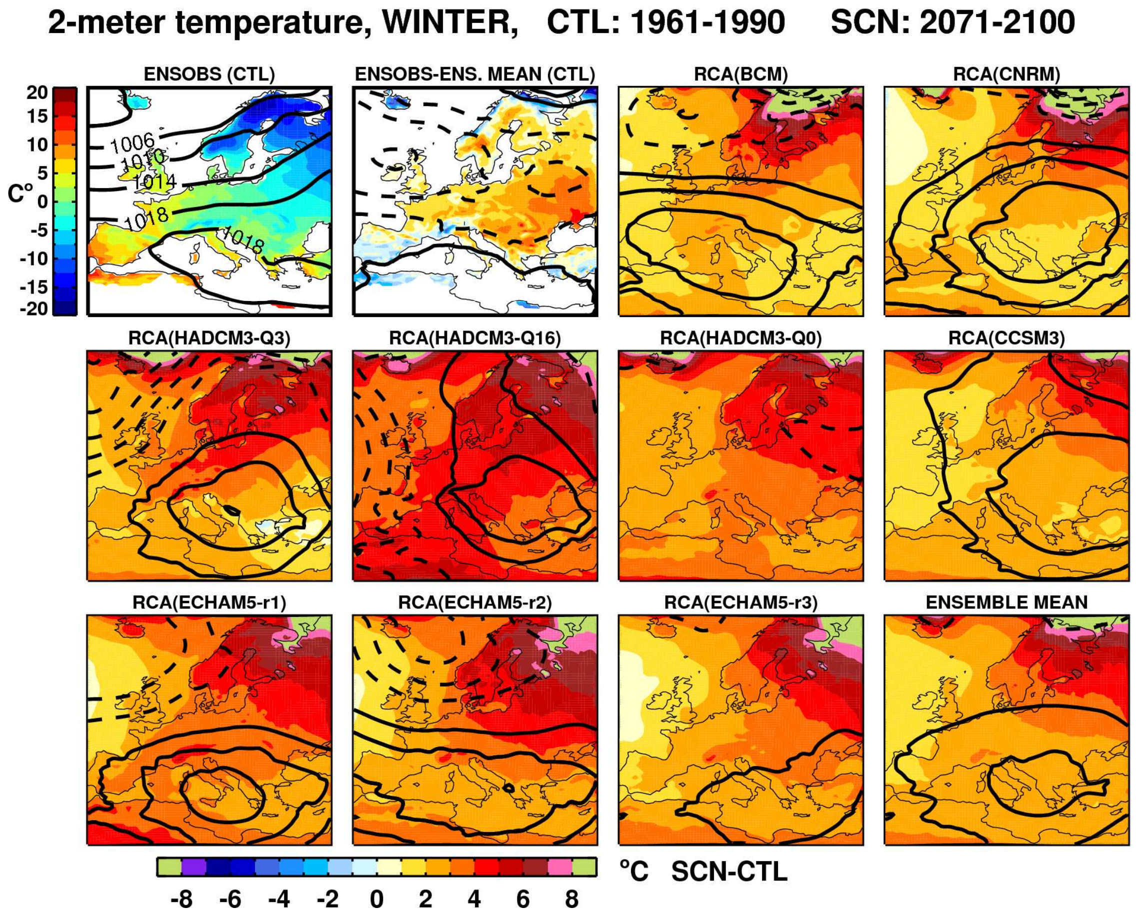

Figure 2. *Change in 2m-temperature and mean sea level pressure (contours) between 2071-2100 compared to 1961-1990. The uppermost two panels to the left shows the ENSEMBLES project gridded observational 2m-temperatures (Haylock et al. 2008) and the ENSEMBLE mean bias from Figure 1. The other panels are results from the individual A1B-simulationsat 50km horizontal resolution listed in Table 1 The mean (lower right) is taken over the ensemble consisting of 5 simulations with different AOGCMs in the two rightmost columns. MSLP changes are shown for every 2 hPa (CTL) and every 1 hPa (SCN-CTL) except 0 (dashed for negative numbers).*

In the relatively near future (2011-2040) indicated in Figure 3 a considerable part of the uncertainty in the climate change signal is related to the natural variability. The three ECHAM5-forced members differ from each other with up to or locally even more than 2°C. These differences are equally large as, or even larger than, the climate change signal at this period. The reason for the large differences is to be found in the large scale circulation in the three ensemble members. The second one displays a strong increase in the north-south pressure gradient over the North Atlantic which leads to excessive warming in northern Europe. This feature is not seen in the other simulations. Also, the HadCM3-forced simulations points in the same direction (Figure 4). In contrast to what one may expect the high climate sensitivity simulation shows a smaller change compared to the lower climate sensitivity simulation. This is also indicative of a strong contribution from natural variability to the overall uncertainty. The MSLP changes depicted in Figure 4 shows that the strong regional response in the low sensitivity simulation is driven by changes in the pressure gradients while the opposite is true for the high sensitivity simulation.

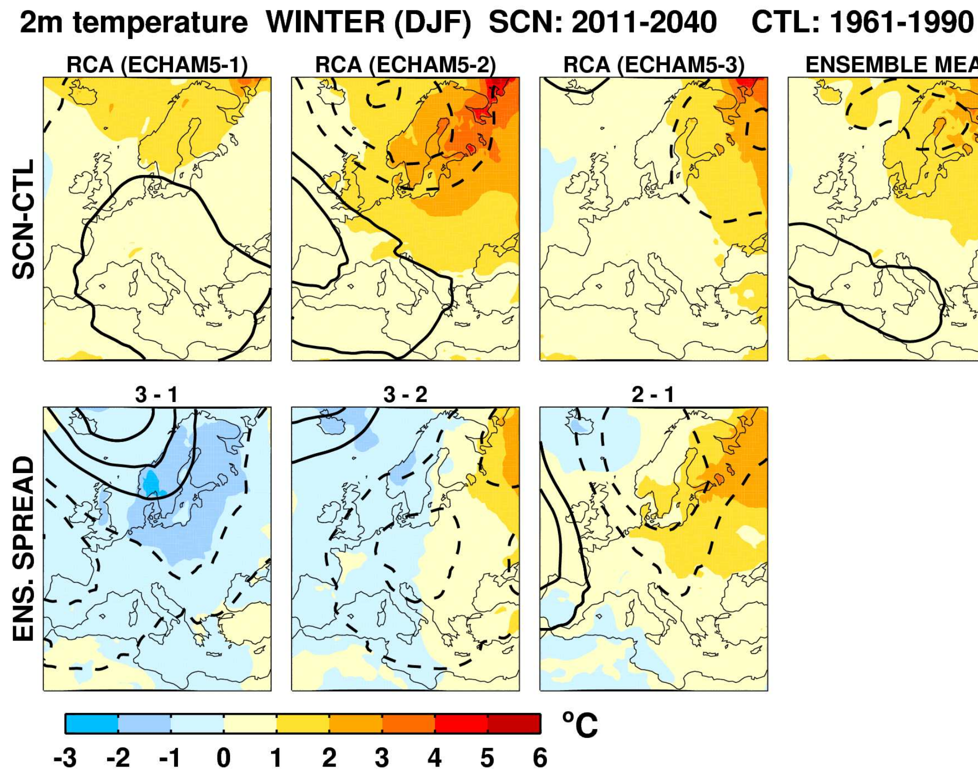

Figure 3. *Changes in winter (DJF) 2m-temperature in 2011-2040 compared to 1961-1990 in the three member A1B-ensemble with ECHAM5 differing in initial conditions on the boundaries. Changes in MSLP are also shown (for ..., -1, -0.5, 0.5, 1, ... hPa).*

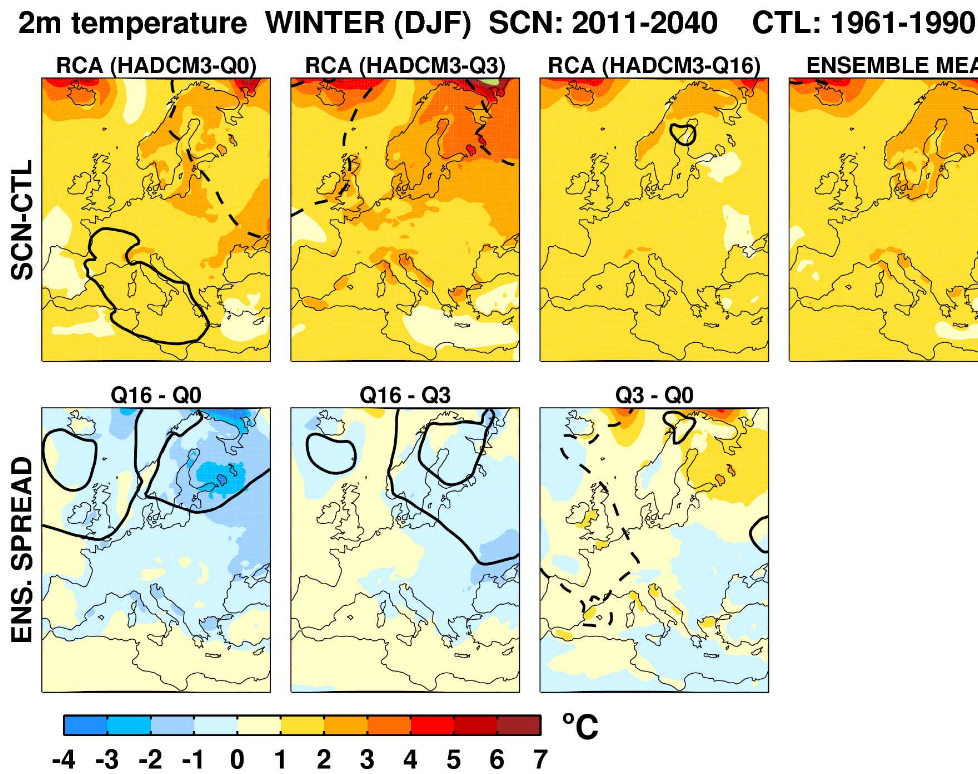

Figure 4. *Changes in winter (DJF) 2m-temperature in 2011-2040 compared to 1961-1990 in the three members A1B-ensemble with the HadCM3 perturbed physics ensemble on the boundaries (rightmost three panels). Changes in MSLP are also shown (for ..., -1, -0.5, 0.5, 1, ... hPa).*

4. Summary and outlook

We report on an ensemble of altogether 17 transient simulations covering the period 1961-2100. All are conducted with the same version of the regional climate model RCA3. Differences between the simulations are that they use different boundary conditions from different AOGCMs operating under several emission scenarios. In addition aspects of natural variability and model uncertainty has been touched upon by downscaling ensembles consisting of simulations with different initial conditions and different formulation of the AOGCM. We have also performed some of the simulations at different horizontal resolution. The main conclusions concerning wintertime temperatures in Europe are:

- There are large differences between the simulations in the recent past climate. These differences are related both to internal variability and to choice of AOGCM. In general these two sources of uncertainty are difficult to distinguish from each other. Here, the three-member ensemble of ECHAM5-driven simulations allows us to look at natural variability alone. Large differences between these three simulations can be seen in some regions but the differences related to choice of AOGCM are generally larger.
- The ensemble mean performs better than most, but not all, individual models for most areas. It is deteriorated by the still limited number of simulations as outliers performing poorly have a relatively large impact on the mean.
- In the relatively near future (2011-2040) we show that a considerable part of the uncertainty in the climate change signal is related to the natural variability. By the end of the century, when the forcing (and the response) is larger, the overall uncertainty is more dominated by the choice of AOGCM and the choice of emission scenario.

5. Acknowledgements

The AOGCM-groups are kindly acknowledged for providing boundary data to us. We acknowledge the E-OBS dataset from the EU-FP6 project ENSEMBLES (http://www.ensembles-eu.org) and the data providers in the ECA&D project (http://eca.knmi.nl). Some of the simulations have been made possible through the ENSEMBLES project funded by the EC through contract GOCE-CT-2003-505539 and some by the Climate and Energy Systems project (CES) funded by the Nordic Research Council. Part of the analysis work has been made within the Swedish Mistra-SWECIA programme. Many of the model simulations with the regional climate model were performed on the climate computing resource Tornado funded with a grant from the Knut and Alice Wallenberg foundation.

References

Bleck R., Rooth C., Dingming H. and Smith L. T., 1992. *J. Phys. Oceanogr.* **22**, 1486-1505.

Christensen, J.H., B. Hewitson, A. Busuioc, A. Chen, X. Gao, I. Held, R. Jones, R.K. Kolli, W.-T. Kwon, R. Laprise, V. Magaña Rueda, L. Mearns, C.G. Menéndez, J. Räisänen, A. Rinke, A. Sarr and P. Whetton, 2007: Regional Climate Projections. In: Climate Change 2007: *The Physical Science Basis. Contribution of Working Group I to the Fourth Assessment Report of the Intergovernmental Panel on Climate Change* [Solomon, S., D. Qin, M. Manning, Z. Chen, M. Marquis, K.B. Averyt, M. Tignor and H.L. Miller (eds.)]. Cambridge University Press, Cambridge, United Kingdom and New York, NY, USA.

Collins, W. D., Bitz, C. M., Blackmon, M. L., Bonan, G. B., Bretherton, C. S., Carton, J. A., 30 Chang, S., Doney, C., Hack, J. J., Henderson, T. B., Kiehl, J. T., Large, W. G., McKenna, D. S., Santer, B. D., & Smith, R. D., 2006. *Journal of Climate,* **19**, 2122–2143.

Déqué M., Dreveton, C., Braun, A., and Cariolle, D. (1994): The ARPEGE/IFS atmosphere model. *Clim. Dyn.*, **10**, 249-266.

Déqué, M., et al., 2007. An intercomparison of regional climate simulations for Europe: assessing uncertainties in model projections. *Climatic Change*. 81, 53-70.

Gordon, C.; Cooper, C., Senior, C.A., Banks, H., Gregory, J.M., Johns,T.C., Mitchell, J.F.B., and Wood, R.A. 2000. *Clim. Dyn.* **16,** 147–168.

Haylock, M.R., N. Hofstra, A.M.G. Klein Tank, E.J. Klok, P.D. Jones, M. New. 2008. *J. Geophys. Res (Atmospheres)*, **113**, D20119, doi:10.1029/2008JD10201.

Hourdin, F., et al., 2006: The LMDZ4 general circulation model: Climate performance and sensitivity to parameterized physics with emphasis on tropical convection. *Clim. Dyn*., 27, 787–813.

Jungclaus J.H., Botzet M., Haak H., Keenlyside N., Luo J.-J., Latif M., Marotzke J., Mikolajewicz U. & Roeckner E., 2006. *J. Clim.* **19**, 3952–3972.

Kjellström, E., et al., 2005. A 140-year simulation of European climate with the new version of the Rossby Centre regional atmospheric climate model

(RCA3). Reports Meteorology and Climatology, 108, SMHI, SE-60176 Norrköping, Sweden, 54 pp.

Lind, P., and Kjellström, E., 2008. Temperature and precipitation changes in Sweden; a wide range of model-based projections for the 21st century. *Reports Meteorology and Climatology*, 113, SMHI, SE-60176 Norrköping, Sweden, 50 pp.

Meehl, G.A., et al., 2007. Global Climate Projections. In: Climate Change 2007: The Physical Science Basis. Contribution of Working Group I to the Fourth Assessment Report of the Intergovernmental Panel on Climate Change [Solomon, S., et al. (eds.)]. Cambridge University Press, Cambridge, United Kingdom and New York, NY, USA.

Murphy, J. M., et al., 2007. A methodology for probabilistic predictions of regional climate change from perturbed physics ensembles. *Phil. Trans. R. Soc. A*, 365, 1993-2028.

Nakićenović, N., et al., 2000. Emission scenarios. A Special Report of Working Group III of the Intergovernmental Panel on Climate Change. Cambridge University Press, 599 pp.

Roeckner E., Brokopf R., Esch M. Giorgetta M. Hagemann S. Kornblueh L. Manzini E. Schlese U. & Schulzweida U. 2006. *J. Clim.*, **19**, 3771–3791.

Royer, J.-F., D. Cariolle, F. Chauvin, M. Déqué, H. Douville, R.M. Hu, S. Planton, A. Rascol, J.-L. Ricard, D. Salas y Mélia, F. Sevault, P. Simon, S. Somot, S. Tytéca, L. Terray, S. Valcke (2002): *C. R. Geophys.*, **334**, 147-154.

Uppala S.M., et al., 2005. The ERA-40 reanalysis. *Q. J. Roy. Meteorol. Soc*. **131**, 2961-3012.

6. First Regional Arctic Climate Scenarios with coupled RCAO

by Torben Königk, Ralf Döscher, Klaus Wyser and Markus Meier

Global climate models show large discrepancies in predictions of present and future climate in the Arctic, and consequently, large uncertainties. In order to complete the puzzle of future Arctic climate change and analyze the mechanisms and impacts, a number of regional Arctic scenario experiments are performed with the Rossby Centre Atmosphere Ocean climate model (RCAO).

A1B scenario simulations of the last IPCC Assessment Report from the Norwegian Bergen Climate Model (BCM) and the German Max-Planck-Institute climate model (ECHAM5/MPI-OM) are used to force the atmosphere at the lateral boundaries of the RCAO model. The ocean boundaries are prescribed using climatological values. Two different regional simulations have been done with forcing from each of the global models. These two simulations differ in the treatment of the surface salinity in the Arctic. To prevent artificial drift, a salinity restoring to 20^{th} century climatology is used in the first run (ECHstand, BCMstand). The second run uses a constant salinity flux correction (ECHflux, BCMflux) which allows for more realistic salinity changes and variability in the future. The results are compared to each other and to the original data of the global models (ECH_GCM, BCM_GCM).

The ECHAM5/MPI-OM forced runs show lower summer sea ice extents and a stronger decrease than the BCM forced runs (Fig. 1). Furthermore, the regional ECHAM5/MPI-OM runs give a lower ice extent than ECH_GCM. Also, the interannual to decadal variability is higher in ECHstand and ECHflux with several periods of low summer ice extent and partial recovery thereafter. Around 2040, the summer sea ice has almost disappeared for the first time and from 2060 on, summers are always almost without sea ice in the Arctic. The regional BCM forced simulations and also BCM_GCM show a much slower sea ice reduction due to a much colder Arctic climate in BCM_GCM. While the sea ice starts to disappear from the southern sea ice edges particularly in the Barents Sea, sea ice thickness decreases more uniformly in the entire Arctic Ocean. The regional models and BCM_GCM tend to have the largest reductions along the Siberian coast while ECH_GCM has largest reductions in the Canadian Archipelago.

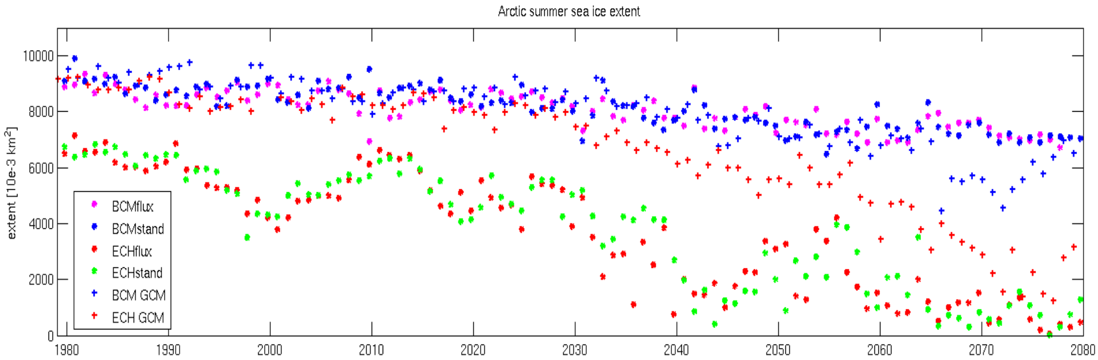

Figure 1. *Arctic summer sea ice extent for the regional simulations and the original global simulations.*

Figure 2 shows the changes in 2 m air temperature in the period 2020-2040 in comparison to the period 1980-2000. The temperature increase is most pronounced in the Barents Sea where sea ice reduction is particularly large. The warming in the Arctic in the regional ECHAM5/MPI-OM forced simulations is larger than in the global simulation and already in 2020-2040 most of the Arctic shows a warming of more than 2 Kelvin. Additionally, both BCMflux and ECHflux respond stronger than BCMstand and ECHstand, respectively. SLP is reduced in the entire Arctic with a maximum in the Barents Sea (not shown). Again, the reduction is most pronounced in BCMflux and ECHflux.

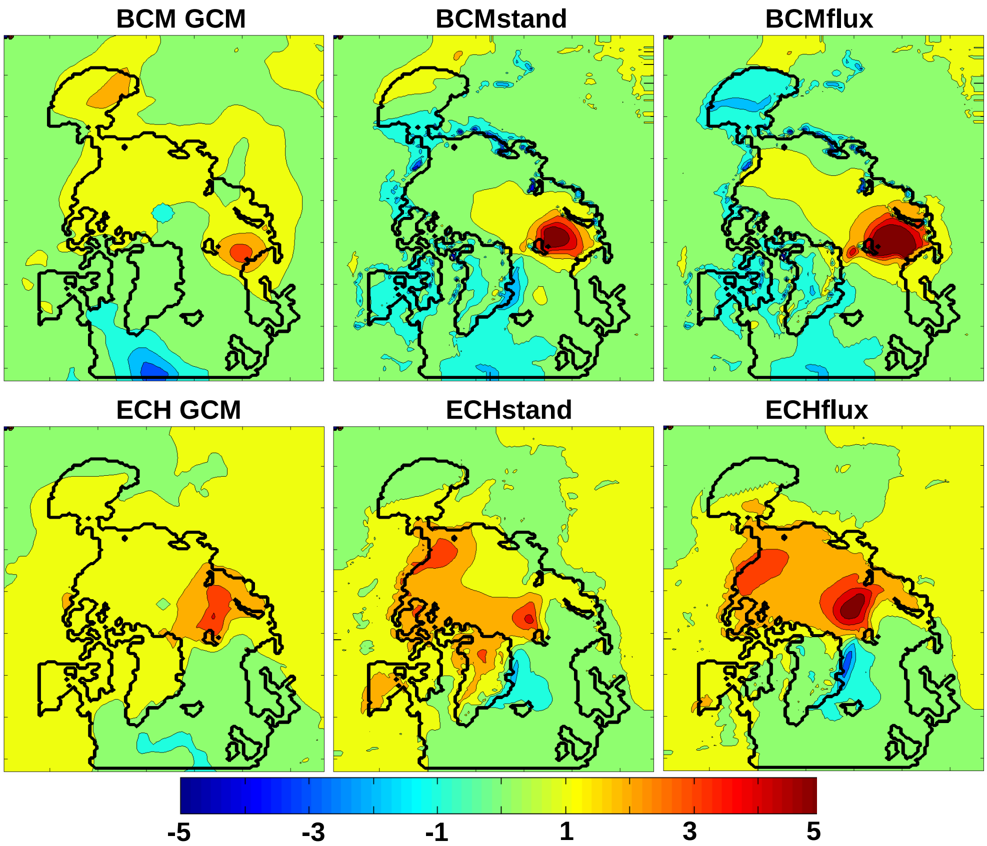

Figure 2. *Annual mean change of 2m air temperature (in Kelvin) between the periods 2020-2040 and 1980-2000 in the regional and the global simulations.*

Summarizing, first results from the regional scenario downscaling experiments show a larger sensitivity and particularly a stronger local response in the Arctic climate to increased greenhouse gas concentrations than in the respective global simulations. The enhanced warming signal in the flux-corrected experiments indicates an influence of sea surface salinity on the change processes. Further scenario downscaling experiments will be carried out in order to quantify uncertainties of Arctic climate change and attribute unequal behaviour of different models.

7. Performance of RCA3 and RCA3.5 over South America

by Anna Sörensson and Patrick Samuelsson

The EC financed projects CLARIS 1 (2004-2007) and CLARIS LPB (2008-2012, http:/www.claris-eu.org) aim at strengthening the collaboration between European and South American institutes and to assess climate change, variability and extremes as well as impacts and adaptation to climate change over South America. Dynamic downscaling is one of the central workpackages in the two projects, providing climate change scenarios for impact studies. Rossby centre was an external collaborator of CLARIS 1, and is a partner of the CLARIS LPB project.

CLARIS 1 was a multidisciplinary pilot project mainly aiming at strengthening the collaboration between institutions from Europe and South America, creating common research strategies (Boulanger et al. 2009). The dynamic downscaling work package aimed at setting up a methodology for model intercomparison and validation of regional climate model performance over South America. Within the context of this project, Rossby Centre carried out simulations with RCA3-E in collaboration with the Argentinean partner CONICET. RCA3-E is a version of RCA3 with modified atmospheric physics and with the land surface database ECOCLIMAP (Masson et al. 2004), to improve the performance over tropical regions. Two time slices of present and future climate (1980-99 and 2080-99) were simulated with ECHAM5/MPI-OM as the forcing AOGCM, and present climate was validated using ERA40 boundaries (Sörensson et al. 2009a). Furthermore, land surface – atmosphere interaction experiments were carried out (Sörensson et al. 2009b).

The CLARIS LPB dynamic downscaling work package aims at generating climate change scenarios for near and far future with a focus on hydroclimate over the la Plata Basin (central and northern Argentina, Uruguay, Paraguay and southern Brazil). The methodology for intercomparison between regional models follows projects like PRUDENCE and ENSEMBLES, although comprising a smaller ensemble of models. Rossby Centre will contribute by generating regional climate change scenarios with a high resolution nesting over la Plata basin with RCA3.5 (Jones et al., this newsletter, with the convection scheme KF instead of BKF).

Here we present the differences between RCA3-E with 24 vertical levels and RCA3.5 with 24 and 40 vertical levels respectively. The models were ran for a test period of 1997-2001 forced by ERA-interim, with one year of spin-up. The model domain and the regions used for calculation of the annual cycle of open land 2m temperature and precipitation are shown in Figure 1. The annual cycles of open land 2m temperature and precipitation for these regions are shown in Figures 2 and 3.

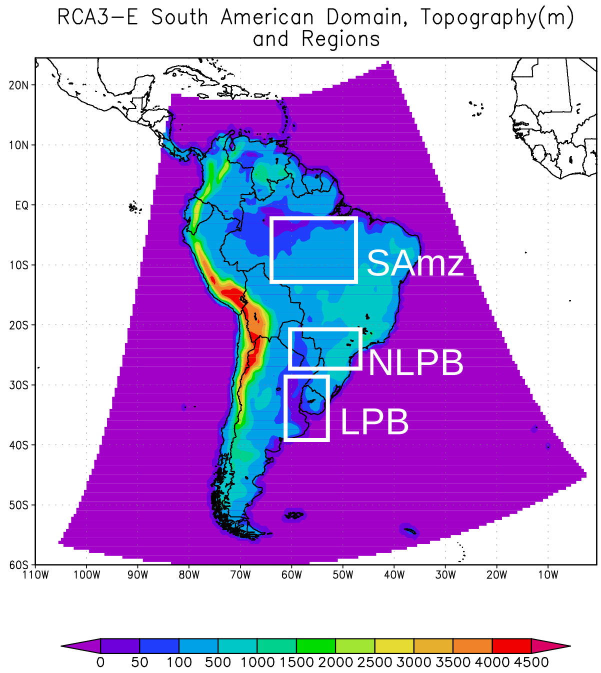

Figure 1. *Domain and regions: Southern Amazonia (SAmz), Northern la Plata basin (NLPB) and la Plata basin (LPB).*

For all regions, RCA3-E has a warm bias for the spring and early summer season (September through December). These biases are mitigated in both RCA3.5 versions, with the 40-levels version closer to observations than the 24-levels version. In the Southern Amazon region, RCA3-E has a cold bias for the JJA season, which is not present in the RCA3.5 version. RCA3-E has dry bias for all three regions and seasons, especially during fall to early spring (April through September).

In the Southern Amazon region, this bias is reduced in RCA3.5, although a small winter bias is still present. In the Northern la Plata region the precipitation is better represented during summer in RCA3.5, but in both la Plata basin regions, the RCA3.5 only mitigates the winter biases slightly. However, in RCA3-E the winter dry bias produced a warmer temperature bias during spring since the soil was dried out.

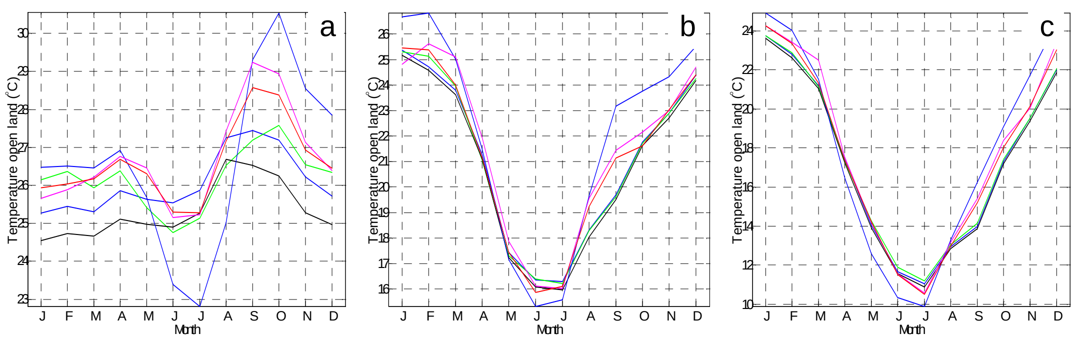

Figure 2. *Annual cycle of open land temperature for a: SAmz, b: NLPB and c: LPB. Dashed lines: green – CRU, blue – ERA40, black – ERA interrim. Continous lines: blue – RCA3, mangenta – RCA3.5 24 vertical levels, red – RCA3.5 40 vertical levels.*

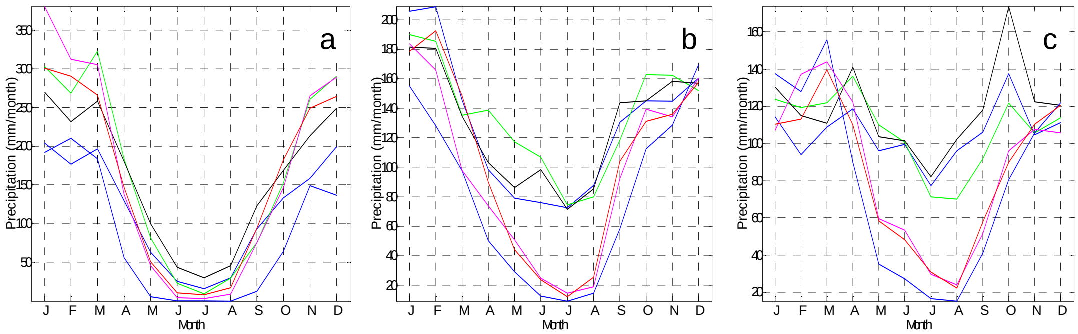

Figure 3. *Annual cycle of precipitation. Regions and colours as in figure 2.*

The temperature biases for spring (SON) are shown in figure 4. In RCA3.5 the soil does not dry out as much in the la Plata region, probably due to the improved land surface scheme together with changes in the cloud cover parameterization.

From the comparison of the model versions it is clear that RCA3.5 simulates a better climate over South America than RCA3-E. The 40 levels version also has a more realistic representation than the 24 levels version of seasonal precipitation over the whole continent (not shown). This is probably due to a more realistic temporal and spatial triggering of convection since the vertical temperature and moisture profiles are better resolved. However, the winter dryness in the la Plata basin is still present, and will be investigated in detail. The moisture transport to the region is mainly supplied by the South American Low Level Jet (SALLJ) that brings moisture to the region from lower latitudes (Vera et al. 2004). If the SALLJ is too weak, a possible reason could be that the transient cyclonic perturbations are too weak, since they modulate the strength of the jet (Liebmann et al. 2004).

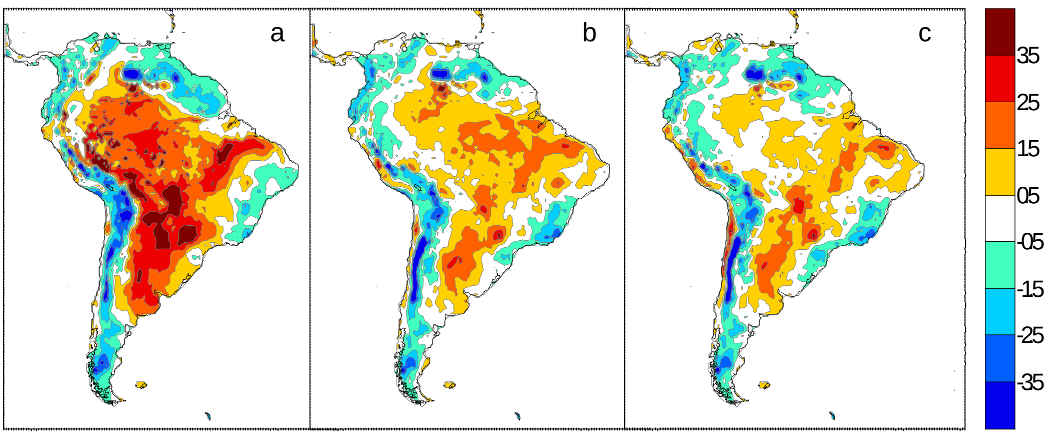

Figure 4. *Open land temperature biases (model – CRU) for the SON season for a: RCA3, b: RCA3.5 (24 vertical levels) and c: RCA3.5 (40 vertical levels).*

References

Boulanger J.-P., G. Brasseur, A. Carril, M. Castro, N. Degallier, C. Ereño, H. Le Treut, J. Marengo, C. Menéndez, M. Nuñez, O. Penalba, A. Rolla, M. Rusticucci and R. Terra, 2009: The European CLARIS Project: A Europe-South America Network for Climate Change Assessment and Impact Studies. Accepted for publication in *Climatic Change.*

Liebmann B., G. N. Kiladis, C. S. Vera , A. C. Saulo and L. M. V. Carvalho, 2004: Subseasonal Variations of Rainfall in South America in the Vicinity of the Low-Level Jet East of the Andes and Comparison to Those in the South Atlantic Convergence Zone. *Journal of Climate*, **17**: 3829–3842.

Masson V., J.-L.Champeaux, F. Chauvin, C. Meriguet and Lacaze, R., 2003: A global database of land surface parameters at 1-km resolution in meteorological and climate models. *J. Climate* **16**(9): 1261–1282.

Sörensson A.A., R Ruscica, C.G. Menéndez, P. Alexander, P. Samuelsson, U. Willén and U. Hansson, 2009a: South America's Present and Future Climate as Simulated by the Rossby Centre Regional Atmospheric Model, 9th International Conference on Southern Hemisphere Meteorology and Oceanography.

Sörensson A.A., C.G. Menéndez, P. Samuelsson, U. Hansson, 2009b: Soil-precipitation feedbacks during the South American Monsoon as simulated by a regional climate model. Accepted for publication in *Climatic Change.*

Vera C., J. Baez, M. Douglas, C. B. Emmanuel, J. Marengo, J. Meitin' M. Nicolini, J. Nogues-Paegle, J. Paegle, O. Penalba, P. Salio, C. Saulo, M. A. Silva Dias, P. Silva Dias, and E. Zipser, 2004: The South American Low-Level Jet Experiment. *Bulletin of the American Meteorological Society*, **87**: 63–77.

8. Simulating Precipitation over Africa with a new version of RCA

by Colin Jones, Grigory Nikulin, Anders Ullerstig, Patrick Samuelsson and Ulrika Willén

1. Introduction

As mentioned on page XX of this newsletter, the international Regional Downscaling Community is aiming to develop a large matrix of Regional Climate scenarios covering Africa to support impact and adaptation work on the African continent. This effort is particularly targeted for the next Assessment Report of the Integovernmental Panel on Climate Change (IPCC), targeted for release in 2014.

In preparation for this activity at the Rossby Centre we are testing a new version of the RCA model over Africa (RCA3.5) by downscaling the new ERA-Interim reanalysis using a model domain encompassing the entire African continent at a horizontal resolution of 0.44°. Integrations have been performed for the period 1995 to 2007. Results are presented here for the period 1997 to 2007, with an emphasis on the ability of the model to capture some of the main observed features of precipitation variability over Africa. The model version RCA3.5 builds on the earlier version RCA3 (Kjellström etal. 2005, Jones etal. 2004) with a number of modifications to enable the model to be more globally applicable. Of particular relevance is that the RCA3 Kain-Fritsch (KF) convection scheme (Kain and Fritsch 1990) has been replaced by the Bechtold-Kain-Fritsch (BKF) scheme (Bechtold etal. 2001). In contrast to the original KF scheme, the BKF scheme treats shallow and deep convection separately allowing different trigger functions and closure schemes to be applied to each physical process. A number of extensions have been made to the original BKF scheme, these are detailed in Jiao and Jones (2008). The other main difference in comparison to the majority of earlier RCA3 integrations is that the number of vertical levels used in the model has been increased for 24 to 40 levels, with a particular increase in vertical resolution near the surface.

2. Model Domain and Analysis Methods

Figure 1 illustrates the integration domain used in these runs, which includes the entire African continent plus surrounding water bodies. In this article we assess the ability of RCA3.5 (hereafter referred to as RCA) to represent precipitation variability over a number of different regions on the African continent with different annual cycles of precipitation. As a first step we present maps of the climatological precipitation for the period 1997-2007 inclusive. We then go onto analyse the annual cycle of precipitation spatially averaged over a number of regions schematically outlined in Figure 1. These include spatially averaged annual cycles for the following regions:

1. 10°W to 10°E, 5°N-15°N; *West Africa/Sahel Region*

2. 10°E to 25°E, 0°N-10°N; *Central Africa, Northen Hemisphere*

3. 10°E to 25°E, 0°S-10°S; *Central Africa, Southern Hemisphere*

4. 25°E to 35°E, 10°S-20°S; *East Africa Highlands, Southern Hemisphere*

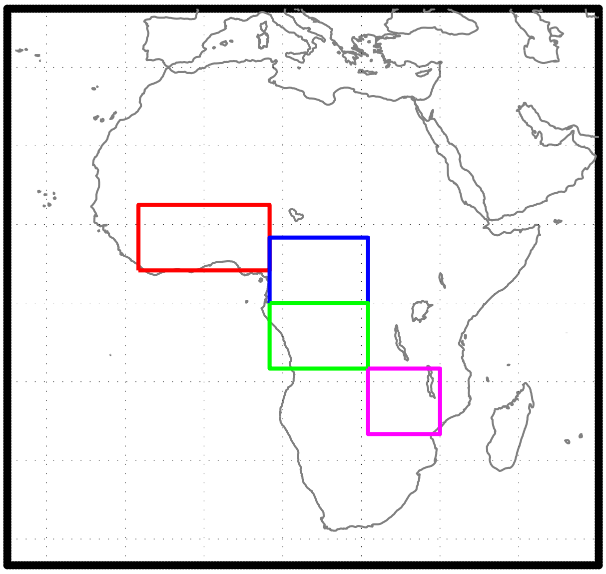

Figure 1. *RCA3.5 model domain, plus the 4 regions used for spatial averaging presented in figure 4.*

Each of these regions has a distinctly different annual cycle of precipitation, as a result of either differing geographical location in relation to the annual cycle of solar forcing, underlying surface type/orography and/or differing atmospheric dynamics controlling the main precipitation mechanisms. In addition to an annual cycle analysis, for regions 1 and 4 we take the longitudinally averaged precipitation and plot the latitudinal progression of precipitation for these 2 regions as a function of time over the full 10 years of the analysis period. Simulated precipitation is compared to satellite observations from the Global Precipitation Climatology Project 1° Daily Accumulated data set (hereafter referred to as GPCP) (Huffman etal. 2001). For consistency all RCA results were interpolated to the 1° regular grid of the GPCP data.

3. Results

3.1 Climatological Mean Precipitation

Figures 2 and 3 show the climatological average precipitation for seasons December-January-February (DJF) and June-July-August (JJA) as simulated by RCA and from the GPCP observations. In DJF precipitation is mainly located over South Eastern Africa and the island of Madagascar. The main structure of the precipitation belt is captured by RCA but there is a clear positive bias over the mountains of East Africa. This appears to be associated with too active convective precipitation in this region, likely resulting from too frequent triggering of convection over the mountains. It is also possible that a portion of this error results from the relatively low resolution of the GPCP data (1° resolution), which might lead to this dataset missing localized regions of extreme precipitation. To address this point we plan to extend our analysis using the Tropical Rainfall Measuring Mission (TRMM) precipitation data which has a spatial resolution of 0.25° (Huffman et al. 2007). While RCA correctly simulates a maximum in precipitation over Northern Madagascar in DJF, the intensity in this region is clearly underestimated. Minima in precipitation are well captured along the west coast of southern Africa and the entire Northern Hemisphere, with an increase in precipitation along the Atlas Mountains, at the extreme north-west coast of Africa.

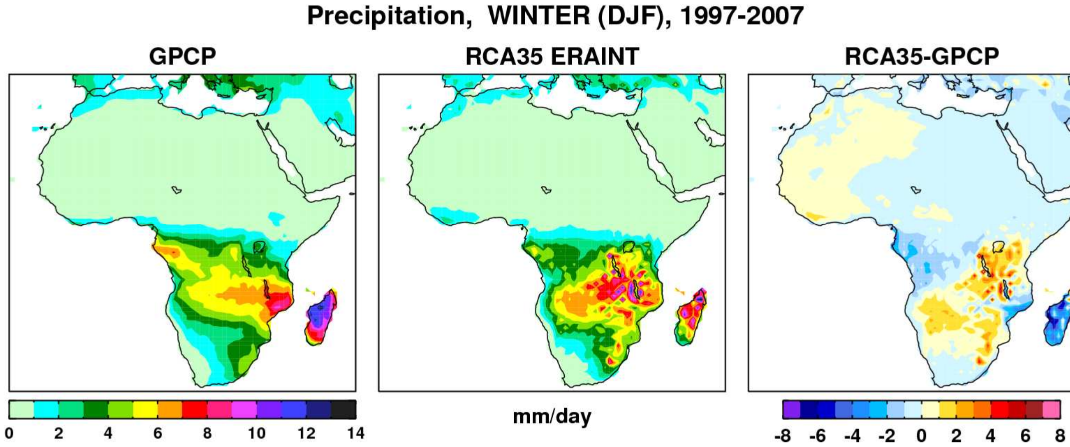

Figure 2. *DJF mean precipitation for the period 1997-2007: GPCP, RCA35 forced by ERA-interim and the difference RCA35-GPCP. All values are in mm/day*

In season JJA the main belt of rainfall moves to the northern hemisphere and is located in the region 5°N to 15°N. The majority of this rain emanates from African Easterly Wave (AEW) systems that generally originate over the Darfur Mountains of Sudan (Kiladis etal. 2006) and then propagate westward, intensifying through a mixed barotropic-baroclinic interaction with the African Easterly Jet (Reed etal. 1977, Holton 1979). AEWs are synoptic scale disturbances with a peak periodicity in the 3-8 day time period (Hodges and Thorncroft 1997) and provide a synoptic scale forcing conducive to the organization of mesoscale convective systems that propagate with the AEW itself (Berry and Thorncroft 2005). GPCP indicates 3 maxima in rainfall along the AEW path, one over the Darfur Mountains and two maxima downstream, where the waves interact with the West African monsoon flow that brings a low level moisture supply from the Atlantic into the wave track. Between Darfur and the Gulf of Guinea a minimum in precipitation can be seen as the AEWs transit a relatively arid region.

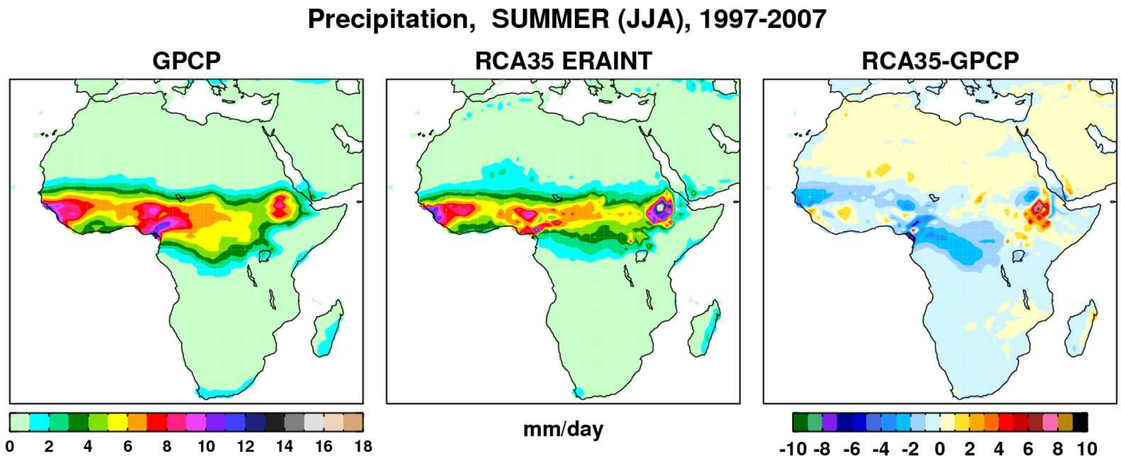

Figure 3. *JJA mean precipitation for the period 1997-2007: GPCP, RCA35 forced by ERA-interim and the difference RCA35-GPCP. All values are in mm/day*

RCA captures these 3 regions of precipitation maxima, suggesting the basic processes controlling the evolution of AEWs are captured by the model. There is a clear positive bias in precipitation over the mountains of Darfur, which is again linked to excessive convective triggering.

3.2 Mean Annual Cycle

Figure 4 shows the mean annual cycle of precipitation, spatially averaged for the 4 regions outlined in section 1. Shown is the annual cycle averaged for the years 1997 to 2007 inclusive, with both daily mean intensities and a 50 day filter passed through the raw daily precipitation data. This filtering is applied both to the observed and simulated data. Over the West African region, north of the equator (figure 4a), RCA3 captures the seasonal cycle of precipitation quite well, although there is a clear overestimate during the onset period of the rainy season (May to June), which can also be interpreted as the rainy season beginning too early in this region (by the order on 1 month). Precipitation rates at the height of the rainy season (July to September) are well simulated as is the decay of the rainy season in October. Figure 4b shows the mean annual cycle further east, over central Africa. In this region RCA shows a better onset date for the rainy season, with a slight underestimate during the main part of the rainy season, again the decay of the rainy season is well captured.

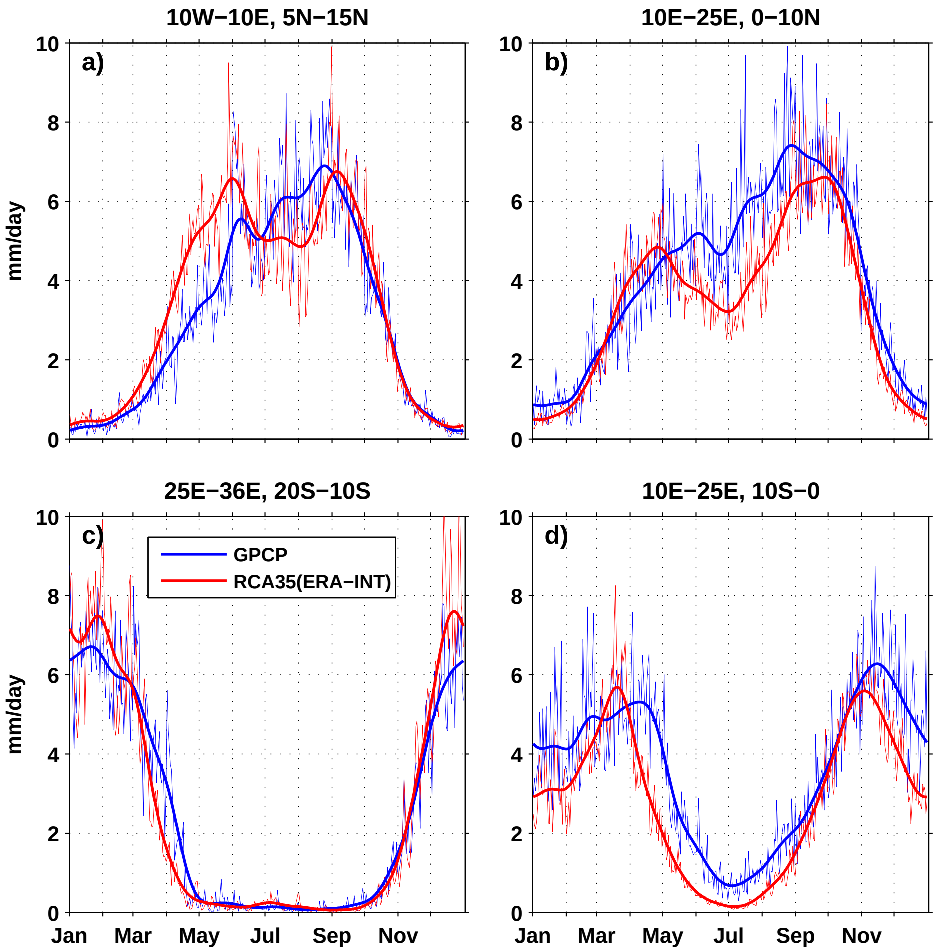

Figure 4. *Spatial Mean Annual Cycle of precipitation for the period 1997-2007 inclusive. Regions over which the spatial average is taken are shown in figure 1 and listed in section 1 of this report.*

Figure 4c shows the mean annual cycle of precipitation over south-east Africa, which is the region of maximum DJF precipitation shown in figure 2. In this region the annual cycle is extremely well captured by RCA, both in terms of timing and absolute magnitude, with moist conditions extending from December through to March, followed by a rapid decrease in precipitation to extreme dry conditions from May to November. Finally, figure 4d shows the mean precipitation for the same longitude region as figure 4b, but averaged south of the equator instead of to the North. A dual peak in precipitation can be seen in the observations, with relative maxima in April and December. This feature is evident in the RCA results also, although the decrease in precipitation between the two maxima is accentuated in the model results. The rainy season is seen to decay in late April in the observations, while in RCA this decay occurs too early. In summary RCA appears to capture the majority of the features of the annual cycle of precipitation in these 4 regions of the African continent.

3.3 Latitudinal Progression of Precipitation and Inter-annual variability

In this section we show the longitudinally averaged precipitation for regions 1 and 4 listed in section 1, plotted as a function of time of year for the 10 years of the analysis period and as a function of latitude. From this one can assess the ability of RCA to represent both the rate and extent of the North-South progression of the main wet and dry periods over these 2 regions, as well as analyse the representation of inter-annual variability in RCA. Figure 5 shows the latitudinal progression of precipitation averaged over the region 10°W to 10°E and concentrates on the northern hemisphere where northward progression is associated with the onset and development of the West Africa monsoon (Vizy and Cook 2001). In both figure 5 and 6, the raw daily precipitation data has been smoothed with a 21 day running mean. Over this region of west Africa the main area of intense precipitation (rates greater than 8 mm/day) propagates northwards from the equator to around 12°N generally over the period March to July, with subsequent southward retreat associated with the decay of the west African monsoon over the period July to October. There is some indication in figure 5 that the observed intense precipitation (greater than 8mm/day) penetrates further north than seen in the RCA results, while weak precipitation rates (less than 2mm/day) penetrate further north in RCA than in observations. With respect to the latter conclusion, one should be aware of the potential limitations of satellite based observations in detecting very low precipitation rates.

The northward propagation of precipitation in RCA during the period March to July appears too rapid in figure 5, consistent with the mean annual cycle for this region shown in figure 4a. Similarly, the southward retreat of the monsoon rains also appears somewhat more rapid than seen in the observations. These caveats aside, the overall annual progression of the West African monsoon is reasonably well captured in RCA, as is the overall intensity of the rainfall. There appears to be little inter-annual variability of the West African monsoon over this period, either in observations or the model results. A longer integration covering at least the period 1960-2007 is likely necessary in order to evaluate the ability of RCA to represent the inter-annual variability of West African rainfall documented in the 1960-1990 period (Nicholson 1980, Janowiak 1988). This is planned for the near future.

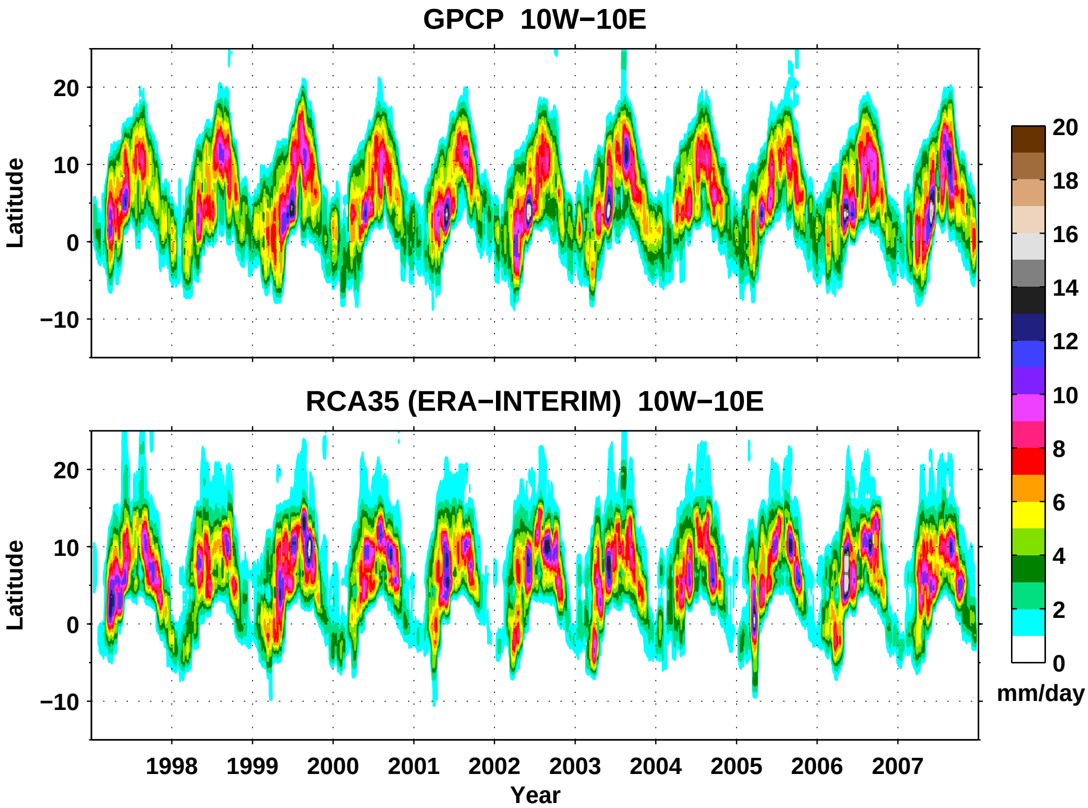

Figure 5. *Latitude-Time cross-section of 21-day running mean precipitation averaged over for 10°W to 10°E. Observations are plotted on the top and RCA results below.*

Figure 6 shows the latitudinal and temporal progression of precipitation averaged over the longitudes 25°E to 36°E. In this region of East Africa there is a weak maximum in precipitation around 10°N during the Northern Hemisphere summer. Rainfall in this region and time of year at ~10°N is associated with African Easterly Wave activity downstream of the Darfur mountains. In figure 2 we showed that precipitation was overestimated in RCA over the Darfur mountains due to excessive convective activity. This will likely result in the AEWs just downstream of Darfur being somewhat more intense than observed, hence explaining the excess rainfall simulated in this region and seen in both figure 2 and in figure 6 at ~10°N.

During the period August to January precipitation is observed to rapidly propagate southwards in figure 6, with significant precipitation penetrating to 20°S by December. Over this longitude belt propagation from the equator to 20°S encompasses the mountain chains of Tanzania and Malawi. RCA accurately captures the rate and extent of the southward propagation, but overestimates the actual precipitation intensities, again likely due to excessive convective activity over the mountainous regions. It is also worth noting that in both figure 5 and 6, areas and time periods of minimal to zero precipitation are well simulated.

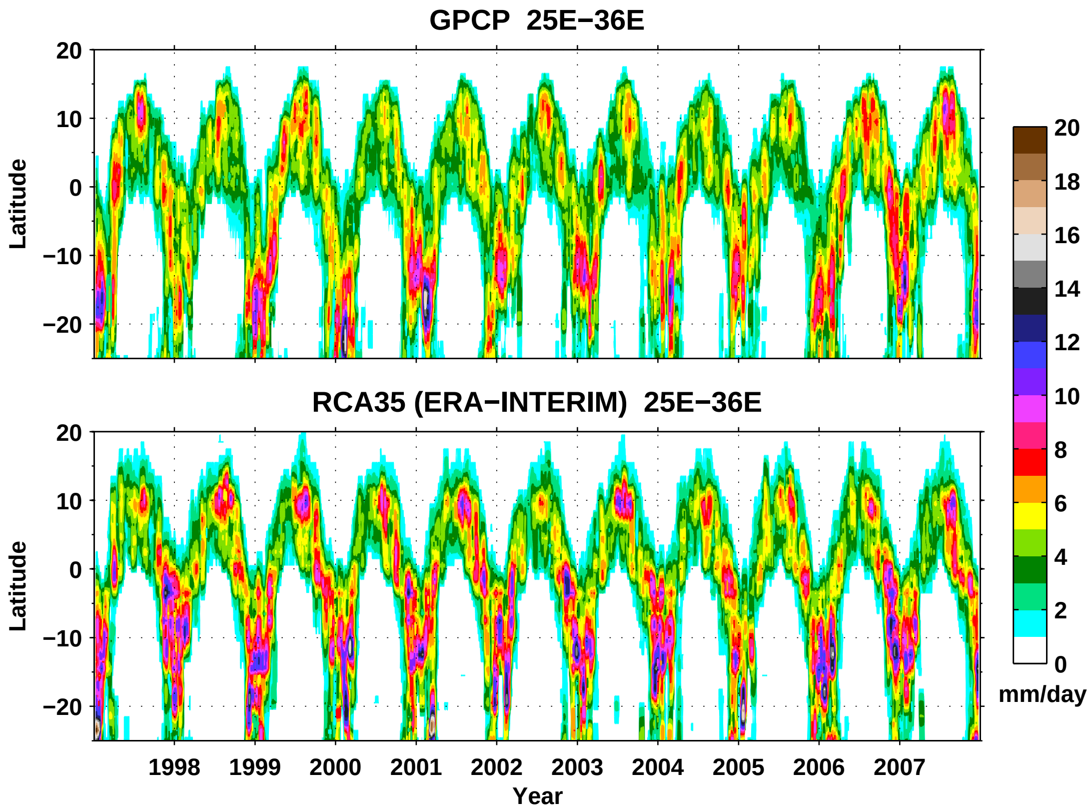

Figure 6. *Latitude-Time cross-section of 21-day running mean precipitation averaged over for 25°E to 36°E. Observations are plotted on the top and RCA results below.*

4. Conclusions

We have analysed the simulated precipitation over Africa from an integration of RCA3.5 forced by ERA-Interim boundary conditions for the period 1997-2007. Our analysis suggests the model captures the majority of the observed components of precipitation over Africa, at least with respect to the annual cycle for a number of locations and the climatological distribution of precipitation across the African continent. The main area of disagreement is that RCA3.5 systematically overestimates precipitation over mountainous regions. While a portion of this overestimate may reflect deficiencies in the resolution of the GPCP observations, we are confident that this overestimate is a genuine model bias. An initial analysis suggests this is related to excessive triggering of convection in these regions. More research is required to fully understand and rectify this problem. The West African monsoon is relatively well captured although both the northward progression and subsequent southward retreat of the monsoon appears to occur somewhat faster than in observations. The period 1997 to 2007 appears too short to analyse the model's ability to represent inter-annual variability of precipitation over Africa. To address this question we are now running RCA3.5 over the same domain for the period 1958 to 2007 using a combination of ERA40 boundary conditions (Uppala etal 2005) and operational ECMWF analyses. Furthermore, the same model domain is being employed to downscale Global Climate Simulations made by the HadCM3 (Gordon etal. 2000) and ECHAM5 (Roeckner et al. 2006) models for the period 1950-2100, based on the A1B emission scenario. Results from these simulations will be reported on subsequently.

References

Bechtold, P.; Bazile, E.; Guichard, F.; Mascart, P. and E. Richard, 2001: A mass-flux convection scheme for regional and global models. Q. R. *J. Meteorol. Soc.,* Vol. 127, 869-886.

Berry, G. and C. Thorncroft, 2005: Case study of an intense African easterly wave, *Mon. Wea. Rev*., 133, 752-766

Gordon, C.; Cooper, C., Senior, C.A., Banks, H., Gregory, J.M., Johns, T.C., Mitchell, J.F.B., and Wood, R.A. 2000. The simulation of SST, sea ice extents and ocean heat transports in a version of the Hadley Centre coupled model without flux adjustments. *Climate Dynamics* 16: 147–168.

Holton J.R. 1979: An Introduction to Dynamic Meteorology (second edition). Academic Press. 391pp.

Huffman GJ, Adler RF, Morrissey MM, et al., 2001, Global precipitation at one-degree daily resolution from multisatellite observations, *J. Hydrometeor*., 2 , 36-50

Huffman, G.J., R.F. Adler, D.T. Bolvin, G. Gu, E.J. Nelkin, K.P. Bowman, Y. Hong, E.F. Stocker, D.B. Wolff, 2007: The TRMM Multi-satellite Precipitation Analysis: Quasi-global, multi-year, combined-sensor precipitation estimates at fine scale. *J. Hydrometeor*., 8, 38-55

Janowiak J.E. 1988: An investigation of interannual rainfall variability in Africa *Journal of Climate* 1, 240-255

Jiao Y and C.Jones 2008: Comparison Studies of Cloud- and Convection-Related Processes Simulated by the Canadian Regional Climate Model over the Pacific Ocean. *Mon Wea Rev* 136,. 4168–4187

Jones, C. G., Willén, U., Ullerstig, A. and Hansson, U. 2004. The Rossby Centre Regional Atmospheric Climate Model Part I: Model Climatology and Performance for the Present Climate over Europe. *Ambio* 33:4-5, 199-210.

Jungclaus, J.H., N. Keenlyside, M. Botzet, H. Haak, J.-J. Luo, M. Latif, J. Marotzke, U. Mikolajewicz und E. Roeckner, 2006: Ocean circulation and tropical variability in the coupled model ECHAM5/MPI-OM. *J. Climate*, 19, 3952-3972

Kain J.S and M.J.Fritsch 1990 A One-Dimensional Entraining/Detraining Plume Model and Its Application in Convective Parameterization. *J. Atmos Sci* 47, 2784–2802

Kiladis, G.N., C.T. Thorncroft and N.M.J. Hall, 2006: Three dimensional structure and dynamics of African Easterly Waves, part I: Observations. *J. Atmos. Sci*., 63, 2212-2230.

Kjellström, E., Bärring, L., Gollvik, S., Hansson, U., Jones, C., Samuelsson, P., Rummukainen, M., Ullerstig, A., Willén U. and Wyser, K., 2005. A 140-year simulation of European climate with the new version of the Rossby Centre regional atmospheric climate model (RCA3). *Reports Meteorology and Climatology* 108, SMHI, SE-60176 Norrköping, Sweden, 54 pp

Nicholson S.E. 1980: The nature of rainfall fluctuations in subtropical West Africa *Mon. Wea. Rev*. 108, 473-487

Reed R.J, D.C.Norquist and E.E.Recker 1977: The structure and properties of African wave disturbances as observed during Phase III of GATE. *Mon. Wea. Rev*. 105, 317-333

Roeckner, E., R.Brokopf, M.Esch., M.Giorgetta, S.Hagemann, L.Kornblueh, E.Manzini, U.Schlese, U.Schulzweida, 2006. Sensitivity of Simulated Climate to Horizontal and Vertical Resolution in the ECHAM5 Atmosphere Model. *Journal of Climate* 19 3771–3791.

Vizy E.K and K.H.Cook 2001: Mechanisms by which Gulf of Guinea and eastern North Atlantic sea surface temperature anomalies can influence African rainfall. *Journal of .Climate* 14, 795-821.

Uppala et al., 2005: The ERA-40 re-analysis. Quart. *J. R. Meteorol. Soc*., 131, 2961-3012.

8. Rossby Centre Staff news

Christer Jansson joined the Rossby Centre in November 2008 to work with land surface - atmosphere interactions. Christer received his PhD 2006 in Environmental Physics from the Royal Institute of Technology, KTH, and he has conducted postdoctoral work at the National University of Singapore.

Marco Kupiainen joined the Rossby Centre in November 2008 as a scientific programmer. Marco held a postdoctoral position at Institut Jean le Rond d'Alembert at Université Pierre et Marie Curie (Paris 6) from 2007 to 2008, working on wall-models coupled with the embedded boundary method for compressible high-speed flows. He received his Tekn Dr from KTH Royal Institute of Technology in 2009.

Anna Lilja joined the Rossby Centre in February 2009 to work on analysis of climate scenarios and external communication. Anna has a M.Sc in meteorology and was formerly head of the Media forecast group at SMHI. She has also worked as a consultant meteorologist and project leader for international programs on Climate Change – Mitigation and Adaptation, and Air Pollution Management.

9. Recent Publications by Rossby Centre Staff

Bärring, L. & Fortuniak, K., 2009: Multi-indices analysis of Scandinavian storminess 1780-2005. *Int. J. Climatol*., DOI: 10.1002/joc.1842

Döscher, R., K. Wyser, H.E.M. Meier, M. Qian, R. Redler, 2009: Quantifying Arctic Contributions to Climate Predictability in a regional coupled Ocean-Ice-Atmosphere Model. *Climate Dynamcis*, 10.1007/s00382-009-0567-y

Graham, L. P., Olsson, J., **Kjellström, E.**, Rosberg, J., Hellström, S.-S. & Berndtsson, R. 2009: Simulating river flow to the Baltic Sea from climate simulations over the past millennium. *Boreal Env. Res*. 14: 173–182.

Jönsson A M, Appelberg G, Harding S, & **Bärring L**, 2009: Spatio-temporal impact of climate change on the activity and voltinism of the spruce bark beetle, Ips typographus. *Global Change Biology*, 15, 486-499, doi: 10.1111/j.1365-2486.2008.01742.x

Kjellström, E. & Lind, P. 2009: Changes in the water budget in the Baltic Sea drainage basin in future warmer climates as simulated by the regional climate model RCA3. *Boreal Env. Res*. 14: 114–124.

Lind, P. & **Kjellström, E**. 2009: Water budget in the Baltic Sea drainage basin: Evaluation of simulated fluxes in a regional climate model. *Boreal Env. Res*. 14: 56–67.

Jörg Stiller and **Uwe Fladrich**: Factorization Techniques for Nodal Spectral Elements in Curved Domains. SIAM *Journal on Scientific Computing*, Volume 30, Issue 5, pp. 2286-2301 (2008)

Uwe Fladrich, Jörg Stiller, and Wolfgang E. Nagel: Improved Performance for Nodal Spectral Element Operators. *International Journal of High Performance Computing Applications*, Vol. 22, No. 4, 450-459 (2008)

Caron, L.-P. and **C. Jones**, 2008: Analysing present, past and future tropical cyclone activity as inferred from an ensemble of Coupled Global Climate Models. *Tellus*, 60A, 80-96.

Graham, L., P., Chen, D., Christensen, O.B., **Kjellström, E.**, Krysanova, V., Meier, H.E.M., Radziejewski, M., Rockel, B., Ruosteenoja, K. and Räisänen, J., 2008. Projections of future climate change. In Assessment of Climate Change for the Baltic Sea Basin. The BACC Author Team. 2008, XXI, 473 p., ISBN: 978-3-540-72785-9.

Jiao Y and **C. Jones** 2008. Comparison Studies of Cloud and Convection Related Processes simulated by the Canadian Regional Climate Model over the Pacific Ocean. *Mon. Wea. Rev*. V136, 11, Nov 2008 P 4168-4187

Karlsson, K., **U. Willén, C. Jones, and K. Wyser** (2008), Evaluation of regional cloud climate simulations over Scandinavia using a 10-year NOAA Advanced Very High Resolution Radiometer cloud climatology, *J. Geophys. Res.*, 113, D01203, doi:10.1029/2007JD008658

Koenigk T. and Mikolajewicz U., 2008. Seasonal to interannual climate predictability in mid and high northern latitude in a global coupled model. *Clim Dyn*, doi:10.1007/s00382-008-0419-1

Koenigk T., Mikolajewicz U., Junglaus J. H., Kroll A., 2008. Sea ice in the Barents Sea: seasonal to interannual variability and climate feedbacks in a global coupled model. *Clim Dyn*, doi:10.1007/s00382-008-0450-2

Markovic M, **C.G. Jones**, P. Vaillancourt , D.Paquin, K.Winger and D.Paquin-Ricard 2008. An evaluation of the surface radiation budget over North America for a suite of regional climate models against surface station observations. *Climate Dynamics*, vol. 31: 779-794.

Moore, K., Pierson, D., Pettersson, K., Schneiderman, E., **Samuelsson, P**. 2008: Effects of warmer world scenarios on hydrologic inputs to Lake Mälaren, Sweden and implications for nutrient loads. Hydrobiologia, 599, 191-199.

Qian M., **C. Jones**, R. Laprise and D. Caya 2008: The Influences of NAO and the Hudson Bay sea-ice on the climate of Eastern Canada. *Climate Dynamics*, 31, 2-3, August 2008.

Tourigny, E. and **C.G. Jones**, 2008: An Analysis of Regional Climate Model Performance Over the Tropical Americas. Part I: Simulating Seasonal Variability of Precipitation Associated with ENSO Forcing. Accepted in *Tellus A* (TeA-08-04-0037.R2).

Zadra, A., D. Caya, J. Côté, B. Dugas, **C. Jones**, R. Laprise, K. Winger and L.-P. Caron, 2008: The next Canadian Regional Climate Model. *Physics in Canada*, Vol. 64., No. 2, Apr-Jun (Spring) Special Issue on Fast Computing.

10. General information

The Rossby Centre works on regional and global climate model development and evaluation, as well as model applications for process studies, climate system studies, climate change research and impact assessment. The Rossby Centre is also involved in a number of EU-funded and other projects on climate modelling and aspects of climate analysis and climate change research. The Rossby Centre newsletter is sent as an email blind copy to those who wish so. Comments and suggestions as to the scope, content and form of the newsletter are welcome. Feedback can be provided via rossby.data@smhi.se